

AD744105

AFML-TR-71-92

SOFT X-RAY BAND SPECTRA AND MOLECULAR ORBITAL
STRUCTURE OF Cr_2O_3 , CrO_3 , CrO_4^{-2} , AND $\text{Cr}_2\text{O}_7^{-2}$

DAVID W. FISCHER

TECHNICAL REPORT AFML-TR-71-92

JULY 1971

Approved for public release; distribution unlimited

AIR FORCE MATERIALS LABORATORY
AIR FORCE SYSTEMS COMMAND
WRIGHT-PATTERSON AIR FORCE BASE, OHIO

Reproduced by
NATIONAL TECHNICAL
INFORMATION SERVICE
U.S. Department of Commerce
Springfield VA 22151

DDC
RECEIVED
JAN 11 1972
RECEIVED

13 C

56

NOTICE

When Government drawings, specifications, or other data are used for any purpose other than in connection with a definitely related Government procurement operation, the United States Government thereby incurs no responsibility nor any obligation whatsoever, and the fact that the government may have formulated, furnished, or in any way supplied the said drawings, specifications, or other data, is not to be regarded by implication or otherwise as in any manner licensing the holder or any other person or corporation or conveying any rights or permission to manufacture, use, or sell any patented invention that may in any way be related thereto.

ACCESSION NO.	
STGT	WHITE SECTION <input checked="" type="checkbox"/>
BDC	BLUE SECTION <input type="checkbox"/>
UNANNOUNCED	<input type="checkbox"/>
JUSTIFICATION	
BY	
DISTRIBUTION/AVAILABILITY CODES	
DIST.	AVAIL. CODE SPECIAL
A	

Copies of this report should not be returned unless return is required by security considerations, contractual obligations, or notice on a specific document.

UNCLASSIFIED

Security Classification

DOCUMENT CONTROL DATA - R & D

(Security classification of title, body of abstract and indexing annotation must be entered when the overall report is classified)

1. ORIGINATING ACTIVITY (Corporate author) Air Force Materials Laboratory Wright-Patterson Air Force Base, Ohio 45433		2a. REPORT SECURITY CLASSIFICATION UNCLASSIFIED	
		2b. GROUP	
3. REPORT TITLE "Soft X-Ray Band Spectra and Molecular Orbital Structure of Cr_2O_3 , CrO_3 , CrO_4^{-2} , and $\text{Cr}_2\text{O}_7^{-2}$ "			
4. DESCRIPTIVE NOTES (Type of report and inclusive dates) Summary Report, November 1969 to January 1971			
5. AUTHOR(S) (First name, middle initial, last name) David W. Fischer			
6. REPORT DATE	7a. TOTAL NO. OF PAGES 49	7b. NO. OF REFS 41	
8a. CONTRACT OR GRANT NO.		9a. ORIGINATOR'S REPORT NUMBER(S) AFML-TR-71-92	
b. PROJECT NO. 7367		9b. OTHER REPORT NO(S) (Any other numbers that may be assigned this report)	
c. Task No. 736702			
d.			
10. DISTRIBUTION STATEMENT Approved for public release; distribution unlimited.			
11. SUPPLEMENTARY NOTES		12. SPONSORING MILITARY ACTIVITY Air Force Materials Laboratory (LPA) Wright-Patterson Air Force Base, Ohio 45433	
13. ABSTRACT A new experimental technique is described whereby the soft x-ray CrL_{III} , CrK , and OK emission and absorption spectra are combined and used to construct empirically a complete molecular orbital diagram for simple chromium-oxygen compounds. All spectral components are assigned specific transitions associated with bonding, antibonding and nonbonding molecular orbitals. In Cr_2O_3 , the spectra indicate that the three outermost electrons have t_{2g} symmetry and are involved in two distinct bonding mechanisms. One of these electrons is localized in a metal-metal covalent bond and the other two are associated with the $\text{Cr-O } \pi$ bond. The results do not support the narrow d-band model which has been proposed for transition metal oxides. For CrO_4^{-2} the deduced MO structure does not agree well with previous calculations and a new interpretation is suggested for the optical absorption spectrum. Contrary to previous assumptions, it is concluded that the highest filled orbital in CrO_4^{-2} is $3t_2$ instead of t_1 . Relationships between the x-ray spectra and various solid state phenomena such as coordination symmetry, bonding distances, valence state, and bonding character are discussed. It is concluded that the x-ray band spectra from compounds are best interpreted on the basis of molecular orbital theory.			

DD FORM 1473
1 NOV 65

UNCLASSIFIED

Security Classification

1

14

KEY WORDS

x-ray
spectroscopy
chromium
molecular-orbitals
band spectra

LINK A

ROLE

WT

LINK B

ROLL

WT

LINK C

ROLE

WT

1a

AFML-TR-71-92

**SOFT X-RAY BAND SPECTRA AND MOLECULAR ORBITAL
STRUCTURE OF Cr_2O_3 , CrO_3 , CrO_4^{-2} , AND $\text{Cr}_2\text{O}_7^{-2}$**

DAVID W. FISCHER

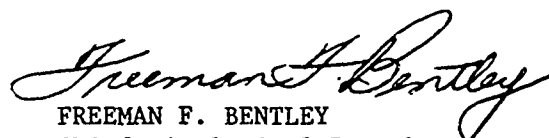
Approved for public release; distribution unlimited

FOREWORD

This report was prepared by the Analytical Branch, Materials Physics Division, Air Force Materials Laboratory, Wright-Patterson Air Force Base, Ohio. The work was initiated under Project 7367, "Research on Characterization and Properties of Materials," Task No. 736702," Physical-Chemical Methods for Materials Analysis," by David W. Fischer, Research Physicist.

This report covers work conducted between November 1969 and January 1971. The report was submitted by the author in April 1971.

This technical report has been reviewed and is approved.



FREEMAN F. BENTLEY
Chief, Analytical Branch
Materials Physics Division
Air Force Materials Laboratory

ABSTRACT

A new experimental technique is described whereby the soft x-ray CrL_{III} , CrK , and OK emission and absorption spectra are combined and used to construct empirically a complete molecular orbital diagram for simple chromium-oxygen compounds. All spectral components are assigned specific transitions associated with bonding, antibonding, and nonbonding molecular orbitals. In Cr_2O_3 the spectra indicate that the three outermost electrons have t_{2g} symmetry and are involved in two distinct bonding mechanisms. One of these electrons is localized in a metal-metal covalent bond and the other two are associated with the $\text{Cr-O } \pi$ bond. The results do not support the narrow d-band model which has been proposed for transition metal oxides. For CrO_4^{-2} the deduced MO structure does not agree well with previous calculations and a new interpretation is suggested for the optical absorption spectrum. Contrary to previous assumptions, it is concluded that the highest filled orbital in CrO_4^{-2} is $3t_2$ instead of t_1 . Relationships between the x-ray spectra and various solid state phenomena such as coordination symmetry, bonding distances, valence state, and bonding character are discussed. It is concluded that the x-ray band spectra from compounds are best interpreted on the basis of molecular orbital theory.

TABLE OF CONTENTS

SECTION	PAGE
I. INTRODUCTION	1
II. EXPERIMENTAL	5
A. Instrumentation	5
B. Dispersing Crystal and Resolution	5
C. Sample Preparation and Spectral Measurement	6
III. RESULTS AND DISCUSSION	8
A. General Comments	8
B. Cr_2O_3	11
C. CrO_4^{-2}	20
D. CrO_3	26
E. $\text{Cr}_2\text{O}_7^{-2}$	26
IV. SUMMARY AND CONCLUSIONS	29
REFERENCES	32
	33

Preceding page blank

ILLUSTRATIONS

FIGURE	PAGE
1. Uncorrected Chromium $L_{II,III}$ Emission and Absorption Spectra from Pure Element and Compounds	42
2. Uncorrected Oxygen K Emission and Absorption Spectra	43
3. Schematic Molecular-Orbital Energy-Level Diagrams for Chromium in Octahedral and Tetrahedral Symmetry Sites With Oxygen Anion	44
4. Empirical Deduction of MO Structure of Cr_2O_3 by Combining the Chromium L, Chromium K, Oxygen K X-Ray Band Spectra	45
5. Empirical Deduction of MO Structure of CrO_4^{-2} by Combining the Chromium L, Chromium K, and Oxygen K X-Ray Band Spectra from Na_2CrO_4	46
6. Comparison of Relative MO Energy Positions of CrO_4^{-2} Determined in This Work and Calculated by Viste and Gray (Reference 35) and Olivari et al. (Reference 36)	47
7. Empirical Deduction of Partial MO Structure of CrO_3 by Combining the Chromium L and Oxygen K X-Ray Band Spectra	48
8. Empirical Deduction of Partial MO Structure of $Cr_2O_7^{-2}$ by Combining the Chromium L and Oxygen K X-Ray Band Spectra from $K_2Cr_2O_7$	49

TABLES

TABLE		PAGE
I	Interatomic Distances in Some Chromium-Oxygen Compounds	34
II	Suggested Electronic Transitions Responsible for Intensity Maxima Observed in Chromium L _{II,III} Emission and Absorption Spectra from Compounds	35
III	Energy Positions of Peak Maxima in Chromium L _{II,III} Emission and Absorption Spectra	36
IV	Suggested Electronic Transitions Responsible for Intensity Maxima Observed in Chromium K and Oxygen K X-Ray Spectra from Chromium-Oxygen Compounds	37
V	Energy Positions of Peak Maxima in Oxygen K Emission and Absorption Spectra	38
VI	Line Widths and Relative Intensities of Unfolds in Cr ₂ O ₃ Band Spectra	39
VII	Relative Percentages of 3d Character in e _g and t _{2g} Valence Orbitals of Cr ₂ O ₃ as Determined from Unfolded CrL _{III} Band Spectrum	40
VIII	Electron Transition Assignments for Two Principle Maxima in Optical Absorption Spectrum of CrO ₄ ⁻²	41

SECTION I

INTRODUCTION

Soft x-ray valence band spectra have for many years been recognized for their potential use in determining the electronic structure of solids. In actual practice, however, the direct utility of the spectra along this line has been severely limited. Over the years many correlations have been made between the spectra from simple compounds and certain physical and chemical properties. Typically, such a correlation will involve a direct relationship between measured wavelength shifts or intensity variations in certain spectral components and a specific property such as bond character, bonding distance, electrical conductivity, heats of formation, and so on. Although these properties are indeed indirect manifestations of the electronic structure of the material, they provide a very incomplete picture of that structure.

Ideally, x-ray band spectra should be capable of yielding a more complete structural picture than this. This expectation arises from the basic origin of the spectra, including both emission and absorption components. X-ray emission bands, according to classical descriptions, are due to electron transitions from the occupied valence/conduction band to an inner level vacancy. Conversely, the absorption spectra are due to the ejection of an inner level electron into one of the available vacant states in the outer regions of the atom. Since it is the structure of these outermost electronic levels that determines the properties of a material, then, so the reasoning goes, the x-ray band spectra should provide us indirectly with all sorts of information about why a material behaves the way it does. Unfortunately, the number of actual cases in which x-ray band spectra have been successfully used in this manner is disappointingly few. There are several reasons for this but in general they can be combined into two problem areas: 1) obtaining reliable band spectra and 2) interpretation of the spectra. It is the intention of this report to focus on these problems (primarily the latter one) for some simple chromium-oxygen compounds such as Cr_2O_3 , CrO_3 , CrO_4^{-2} , and $\text{Cr}_2\text{O}_7^{-2}$.

Compounds of the first-row transition metals are especially interesting from an electronic structure standpoint as reflected in their remarkably varied physical and chemical properties (Reference 1). In attempting to unravel the complexities of the electronic structure of some of the more fascinating compounds in this group, many different types of experiments have been performed. It is a curious fact, however, that x-ray band spectra, despite their potential value in determining significant features of the electronic structure, have been virtually ignored in studying these materials. To be sure, there are problems in obtaining and using the spectra but there are distinct advantages, too. The present author has attempted to indicate this in some recent work on the soft x-ray spectra from some titanium and vanadium compounds (References 2,3,4,5, and 6).

One of the key points in two previous papers (References 4 and 6) has been the use of a molecular orbital (MO) model to interpret the titanium and vanadium $L_{II,III}$ emission and absorption spectra. Recently, several other workers have also recognized the utility of MO theory in explaining certain features of x-ray band spectra which are difficult or impossible to rationalize by any other means (References 7 through 15). There are still those, on the other hand, who claim that MO theory is fine for explaining the bonding in highly covalent materials such as transition metal complexes, but resist any effort to apply it to predominantly ionic materials such as Ti_2O_3 , VO_2 , and Cr_2O_3 or to metal-like compounds such as TiC or VC. Actually, however, MO theory is quite flexible, in that it is capable of describing any degree of covalent-ionic bonding character so that in principle it is perfectly legitimate to apply it to simple inorganics such as oxides, nitrides, and carbides. There is certainly a high degree of interaction between metal atom and nonmetal atom orbitals in these compounds so it seems only reasonable to use a bonding model which takes these interactions into account. If that model is also capable of accurately explaining the myriad of details in the soft x-ray emission and absorption band spectra better than any other model which has been advanced, then it must be worth some consideration. One of the purposes of this report is to demonstrate that the MO model is directly

applicable to chromium-oxygen compounds in which chromium has either a +3 or +6 valence state and occupies either an octahedral or tetrahedral coordination site. The x-ray band spectra will then be used to construct empirically a complete MO energy-level diagram involving both occupied and vacant orbitals within 20eV or so of the Fermi energy. No other experimental technique is capable of doing this.

To empirically determine the complete electronic structure of a transition metal compound, however, one needs more information than is contained in any one emission band or absorption spectrum. The reason for this is rooted in the symmetry characters of the outer orbitals and the dipole selection rules governing x-ray transitions. In forming a compound such as Cr_2O_3 , the 3d, 4s, and 4p levels of the metal atom interact with the 2s and 2p levels of the nonmetal atom. According to MO theory, in which a linear combination of atomic orbitals (LCAO) is used, this interaction will result in a series of bonding and antibonding molecular orbitals such as shown later on in this report (Figure 3). The important point to note here is that these outermost electron levels will consist of admixed s, p, and d symmetries. Now a K x-ray emission band results from transitions of the outermost electrons to a vacancy created in the 1s core level. According to the dipole selection rules only electrons in levels having p symmetry can make such a transition. The K band, therefore, will reflect only the distribution of p symmetry in the outer levels and tell us nothing about the distribution of s and d symmetry. Conversely, the L or M band will reflect the distribution of s and d symmetry but not of p symmetry. Obviously, if we expect to obtain a complete picture of the outer electronic structure it will be necessary to combine the information present in both K and L band spectra. Most x-ray band structure investigations of compounds have not been done from this viewpoint, which makes the information obtained about the band structure very limited in scope. The importance of using the combined spectra has been recently demonstrated by this author for some titanium and vanadium compounds (References 5 and 6). In this report, the following spectra will be used for the chromium-oxygen compounds: chromium L_{III} (valence orbitals $\rightarrow \text{Cr}2p_{3/2}^3$), chromium L_{II} (valence orbitals $\rightarrow \text{Cr}2p_{1/2}^1$),

chromium $K\beta_{2,5}$ (valence orbitals \rightarrow Cr1s), oxygen K (valence orbitals \rightarrow O 1s), and their corresponding absorption spectra.

The investigation of these various band spectra from chromium-oxygen compounds is presented, therefore, with several objectives in mind. The primary objective is to empirically determine the complete outer electronic arrangement and energy positions of the bonding, antibonding, and non-bonding molecular orbitals. Also, the different valence states and coordination numbers of the chromium ion in various compounds should, according to MO theory, result in quite different energy-level arrangements and symmetry character of levels. This, in turn, should cause specific differences to appear in the x-ray band spectra and therefore give a valid indication of whether or not the MO model is capable of accurately explaining all the changes which occur in the spectra. It will be shown that this model is indeed applicable to the chromium-oxygen compounds. The empirical electronic structure obtained will be compared to other types of experimental data and to theoretical calculations, where possible.

It will be seen that the x-ray results do not agree very well with theoretical calculations of the electronic structure in some cases and reasons for the disagreement are suggested. New interpretations will be given for the optical absorption spectra of the CrO_4^{-2} ion based on the x-ray MO structure. In Cr_2O_3 two types of 3d (t_{2g}) electrons are observed and the results do not agree with the very narrow d model proposed elsewhere (References 1 and 16).

SECTION II

EXPERIMENTAL

A. INSTRUMENTATION

The plane single-crystal vacuum spectrometer used to obtain the spectra is the same as described previously (Reference 2). Characteristic x-ray spectra are produced by direct electron beam bombardment of the target material. The interchangeable anode assembly of brass, copper, or aluminum is constructed so that the x-ray takeoff angle is continuously variable between 0 and 90°. A flow-proportional detector with Porvair window and argon-methane flow gas is used at a reduced pressure of 120 Torr. Spectrometer vacuum under normal operating conditions is about 1×10^{-6} Torr.

Wavelength positions of the spectral features measured in this investigation have a probable error of $\pm 0.02\text{\AA}$ ($\pm 0.3\text{eV}$) but wavelength differences could be measured to $\pm 0.005\text{\AA}$ ($\pm 0.1\text{eV}$). The data points on the spectral curves have a statistical deviation of 2-3% at the peak maxima and less than 1% at the tails.

B. DISPERSING CRYSTAL AND RESOLUTION

A rubidium acid phthalate crystal (RAP, $2d=26.118\text{\AA}$) was used in obtaining both the chromium L and oxygen K spectra (Reference 3). The oxygen K bands were also obtained with a clinocllore crystal [$2d=29.393\text{\AA}$ (Reference 2)] to aid in removing the anomalous high energy peak introduced by the RAP crystal (Reference 3).

The effective diffraction pattern of the spectrometer (window width) was tentatively determined although there is not universal agreement on the way to do this for a single plane-crystal spectrometer. The technique used here was to record the $K\alpha_1$ and $K\alpha_2$ lines of V, Cr, Mn, Fe, Co, and Ni in various multiple orders and compare the measured half-widths to the

so-called standard half widths by the expression $W_m^2 = W_\lambda^2 + W_A^2$, where W_m = the half-width of the experimentally measured line, W_λ = the true half-width of the line, and W_A = the half-width of the spectrometer window. For the RAP crystal the instrumental window was calculated to be 0.81eV at the CrL_{III} band maximum (21.7Å) and 0.53eV at the oxygen K band maximum (23.6Å). With the clinocllore crystal the window is 0.94eV at the oxygen K band.

Due to the fact that the window width of the spectrometer varies with the wavelength and that the exact shape of the window is not known, the band spectra shown in this report have not been corrected for instrumental broadening. This is not considered to have any significant effect on the spectral interpretations which are offered.

The chromium K spectra which are used were not obtained by the author but were taken from the literature. The exact literature references are given later in the discussions of specific compounds and these spectra are also uncorrected for instrumental effects.

C. SAMPLE PREPARATION AND SPECTRAL MEASUREMENT

To obtain the emission band spectra, target specimens of Cr_2O_3 were prepared by mixing a fine powder into a slurry with ethanol and painting it in a thin film on the anode surface. Specimens of CrO_3 , the chromates, and dichromates were prepared in a similar fashion except that the slurry liquid was H_2O instead of ethanol. After painting it on the anode surface, the specimen film was dried in air at 120°C, coated with a finely sprayed film of graphite, and placed immediately into the spectrometer vacuum. When prepared in this fashion, all of the compounds, including CrO_3 , remained chemically stable under normal excitation conditions.

Each of the sample materials was obtained from at least two different sources and checked by x-ray diffraction. One of the Cr_2O_3 specimens was a broken segment of a special high-purity single crystal.

Obtaining the x-ray band spectra from these materials involved a tremendous amount of work. For each spectrum shown in this report, at least 20 complete runs were made. These runs were made under a wide variety of excitation conditions by varying parameters such as the bombarding electron beam voltage, the beam current, the sample chamber vacuum, and the length of time that the sample was subjected to the primary electron beam. Before any of the spectra were considered to be truly characteristic of the original sample material, they had to be completely reproducible time after time. All of the chromium L and oxygen K spectra shown here satisfy this requirement. This is important because a typical bombarding electron beam voltage of 3-4kV will only probe the first 100 layers or so below the surface. If any chemical change occurs at or near the surface during the excitation process, the soft x-ray band will not be characteristic of the starting material.

For the chromium L and oxygen K wavelength region it is extremely difficult to make absorption specimens which are both uniform enough and thin enough to transmit the continuum radiation in the usual manner. Successful films were made for only one of the compounds, Cr_2O_3 . This was done by mixing an ultra-fine powder in a dilute solution of parlodion in amyl acetate. An eyedropper was used in depositing a few drops of this mixture on the surface of a shallow pan of water. The drops spread out to form a uniform film which can be picked up on a wire hoop. The film thickness can be varied by the amount of powder mixed in the solvent originally. An optimum thickness was determined by trial and error, and for the CrL_{III} absorption in Cr_2O_3 it was found to be about 0.6 mg/cm^2 .

The CrL_{III} and OK absorption spectra for all of the other materials were obtained by the differential self-absorption method which has been explained previously (References 2 and 3). Although absolute absorption coefficients cannot be obtained from these self-absorption spectra there is the advantage of their being obtained from the same specimens and at the same time as the emission bands. This considerably simplifies the matching of emission and absorption energy scales and provides strong confidence that both types of spectra represent precisely the same chemical state of the target material.

SECTION III

RESULTS AND DISCUSSION

A. GENERAL COMMENTS

The chromium compounds of particular interest in this investigation are the oxides Cr_2O_3 and CrO_3 , the chromates (CrO_4^{-2}), and dichromates ($\text{Cr}_2\text{O}_7^{-2}$). In each of these materials the chromium ion is either octahedrally or tetrahedrally coordinated to the oxygen ligands. In Cr_2O_3 , chromium has a +3 valence and occupies a slightly distorted octahedral site; in CrO_3 , CrO_4^{-2} , and $\text{Cr}_2\text{O}_7^{-2}$, chromium has a +6 valence and is tetrahedrally coordinated. This tetrahedron becomes quite distorted in progressing from CrO_4^{-2} to CrO_3 to $\text{Cr}_2\text{O}_7^{-2}$. As will be shown, this distortion has a significant effect on the x-ray band spectra, and is caused directly by gross variations in the chromium-oxygen and chromium-chromium interatomic distances. The various crystallographic parameters which influence the bonding, and hence the x-ray bands, are summarized in Table I.

The chromium $L_{\text{II,III}}$ emission and absorption spectra from the compounds compared to that from the pure metal are illustrated in Figure 1. Except for the pure Cr spectrum and Cr_2O_3 emission bands, none of these spectra have ever been shown in the literature before. As can be seen, the total band spectrum covers the 550 to 590eV (21.0 to 22.5Å) energy region. Each of the emission bands (solid-line spectra) is subject to serious distortion from self-absorption effects very similar to that shown previously for titanium and vanadium $L_{\text{II,III}}$ bands (References 2,3,5, and 6). Consequently, the bands illustrated in Figure 1 were obtained under conditions of negligible self-absorption, although multiple-vacancy satellite emission is at saturation (Reference 2). The numbers placed on the high-energy tails of the emission bands indicate the bombarding electron beam voltage, beam current, and takeoff angle with which they were obtained. Each of the $L_{\text{II,III}}$ absorption spectra from the compounds (dashed curves) is a self-absorption replica obtained as described previously (References 2,3, and 6).

The pure metal spectrum is included only for reference purposes and will be discussed in detail in a subsequent report.

The oxygen K emission and absorption spectra from these same compounds are shown in Figure 2. Here also, the emission bands (solid curves) were obtained with negligible self-absorption and are uncorrected for broadening effects. Absorption spectra (dashed curves) are self-absorption replicas. The relation between these oxygen spectra and the chromium $\gamma_{I,III}$ and chromium K bands will later be compared in detail for each compound.

In Figures 1 and 2 each of the emission maxima is denoted by a capital letter and each of the absorption maxima by a lower-case letter. The energy positions and relative intensities of these maxima are the basis of the molecular orbital interpretation which will follow. As mentioned earlier, each of the compounds represented in the figures results from different coordination symmetries and/or valence states of the chromium ion. According to MO theory, each of these symmetries should lead to a different interaction between the chromium and oxygen outer orbitals, and therefore produce different MO energy-level arrangements. This in turn should result in specific differences in the x-ray emission and absorption bands and provide a reasonably good test of whether or not the proposed MO interpretation of the spectra is at least qualitatively correct. The interpretation which is offered here follows along the same lines developed previously for titanium and vanadium compounds (References 4, and 6). The derivation and formation of molecular orbitals for various coordination symmetries is textbook information (References 17 and 18) and will not be detailed here. It is of interest, however, to know what type of MO diagram is to be expected, in general, for a transition metal ion in octahedral and tetrahedral symmetry sites. This is indicated schematically in Figure 3. These diagrams are adapted from Ballhausen and Gray's book (Reference 17) and are based on the assumption that the metal ion 3d, 4s, and 4p atomic orbitals interact in the LCAO approximation with the oxygen 2s and 2p orbitals. As such, they are only qualitatively correct but they provide a firm starting point for interpreting the individual x-ray spectra. The idea now is to assign

each x-ray spectral maximum as being due to an electron transition between a specific MO and core level. Actually, this is considerably easier to do for x-ray spectra than for optical spectra because in the x-ray case the inner level is essentially atomic in character and can be considered to have a constant energy value for a given compound. If such MO assignments can be made with a reasonable degree of confidence for both the x-ray emission and absorption spectra then obviously these spectra will form a strong empirical foundation for deducing a complete and accurate molecular-orbital structure for each compound. Since no other experimental technique has been proved capable of doing this, the results could have far-reaching significance as to the virtually untapped potential of the soft x-ray band spectra from compounds.

For the chromium and oxygen band spectra discussed in this report the MO interpretations rely heavily on the usual dipole selection rules. By taking into account the relative peak intensities and their relative energy positions for each spectral series, therefore, we might expect to make reasonably confident assignments for each component. This will be done and explained in detail for each type of compound in the sections which follow. Included with the schematic MO diagrams in Figure 3 are vertical lines indicating which MO's would most likely be expected to contribute to the CrL_{III} and OK spectra. The MO's contributing to the CrL_{III} band contain at least some 3d or 4s admixture while those involved in the OK band contain 2p states. Table II contains the peak assignments for the $\text{CrL}_{\text{II,III}}$ spectra shown in Figure 1. Table III lists the experimentally measured energy positions for these peak maxima. Tables IV and V give comparable data for the oxygen K spectra. These tables will be frequently referred to in the following sections and although the reasoning behind the specific electron transition assignments may not be apparent at this point, it will be later on.

Each of the CrL_{III} and OK band spectra illustrated in the following sections has been unfolded into its constituent components by means of the DuPont Model 310 Curve Resolver. Since complicated spectra can often be resolved into almost as many components as the operator has the patience

to attempt, two basic points were adhered to for the spectra shown here:

- (1) Both Gaussian and Lorentzian unfolds were tried for each spectrum and
- (2) the simplest solution was sought, i.e., the spectra were resolved into as few components as possible. As a result it was found that the CrL_{III} spectra (both emission and absorption) were best approximated by Gaussian components and the OK spectra by Lorentzian components. This was the case for every compound, including many which are not shown in this report. Why the different spectra should unfold into different symmetry components is not clear to the author. Inner levels are generally believed to be Lorentzian in shape while outer levels (molecular-orbitals) are often assumed to have a Gaussian shape (Reference 19). At any rate, whether coincidental or not, the unfolding procedure used here results in precisely the correct number of components predicted by the MO model for both octahedral and tetrahedral compounds. With certain reservations, these unfolded components can be used not only to accurately position the individual electronic orbitals but to give some indication of their width as well.

With these points in mind, let us now proceed to examine the x-ray band spectra from some individual compounds.

B. Cr_2O_3

Cr_2O_3 crystallizes in the corundum structure in which the chromium-oxygen octahedron is slightly distorted (Reference 20). Along the threefold axis the chromium ions (cations) form pairs and are ordered antiferromagnetically up to the Neel temperature of about 45°C (Reference 21). It is an insulator both above and below this temperature. Apparently no calculations have been made of the electronic band structure for Cr_2O_3 but some work has been done on the isostructural compounds Ti_2O_3 and V_2O_3 (References 1, 16, 22, and 23). It will be assumed here that certain features of the band structure for these three sesquioxides (corundum phase) are very similar, the main difference being the number of 3d electrons.

The $\text{CrL}_{\text{II,III}}$ emission and absorption spectra obtained from Cr_2O_3 are shown in Figure 1. According to the dipole selection rules these spectra should reflect primarily the distribution of 3d symmetry in the outermost levels of the compound. Since it is these d electrons that are mainly responsible for many of the important properties (e.g., conductivity, magnetism), the $\text{L}_{\text{II,III}}$ spectra should contain some important information about the structure. It is obvious in Figure 1 that the appearance of the emission band from Cr_2O_3 is considerably different from that of elemental Cr. New components labeled F, A, G, C, D, and E are observed in the oxide but not at all in the pure metal. This is exactly what was observed previously for the $\text{L}_{\text{II,III}}$ bands from titanium and vanadium oxides (Reference 4). The extra components in those oxides were interpreted as being due to the presence of ligand 2p and 2s orbitals and the same explanation is used here for Cr_2O_3 . It will be noticed in Figure 1 that the $\text{L}_{\text{II,III}}$ absorption spectrum does not change as much as the emission band in going from metal to oxide. The exact energy positions of each of the emission and absorption maxima referred to are listed in Table III.

An interpretation of the $\text{L}_{\text{II,III}}$ spectrum from Cr_2O_3 requires we have at hand the CrK and OK band spectra. It is also helpful to refer to the schematic MO energy-level diagram for octahedral symmetry shown in Figure 3. The method of relating the x-ray spectra to the MO structure is illustrated in Figure 4. Shown here are CrL_{III} and OK spectra obtained in this work and CrK band spectrum taken from Menshikov and Nemnonov (Reference 24). The zero of energy is arbitrarily placed at the Fermi energy which is here assumed to be at the CrL_{III} absorption edge. Each of the spectra is positioned on the relative energy scale by lining up peaks b and c in the absorption spectra. The reason for this will become apparent shortly.

As mentioned earlier, the CrL_{III} spectrum has been resolved into Gaussian components and the OK spectrum into Lorentzian components. Before unfolding the L_{III} emission band, everything on the high energy side of the L_{III} absorption edge was subtracted away. It is assumed that any emission components which occur on this side of the edge are

L_{III} multiple ionization satellites and L_{II} band features and can therefore be ignored in determining the MO structure. Also, all the absorption features which occur to the high energy side of maximum d (see Figure 1) are ignored since they are L_{II} absorption transitions involving the same outer orbitals represented by the L_{III} components (see Table II). The Cr spectrum has not been unfolded because it has been replotted from a Russian publication and not enough is known about the experimental conditions used to obtain it.

Now, referring to Figures 3 and 4, let us examine the CrL_{III} emission band. Since this spectrum should reflect primarily the distribution of 3d states we will assume that the main components are due to transitions from the occupied orbitals which contain a significant amount of 3d character. Peaks B, F, and A are therefore assigned as originating in the $2t_{2g}$, $1t_{2g}$, and $2e_g$ MO's respectively. The $2t_{2g}$ orbital is only partially occupied so it should be involved in the absorption spectrum also. In fact, it is assumed that the first two absorption maxima represent the two lowest vacant MO's which are $2t_{2g}$ and $3e_g$. These two orbitals consist mostly of 3d character but there is also expected to be some p character present because of the chromium-oxygen orbital overlap. Indeed, both the CrK and OK absorption spectra contain b and c maxima and it is the alignment of these peaks in all three spectra which dictates their relative positions on the energy scale. In the chromium K emission band the two strongest peaks are assumed to originate in orbitals consisting of some 4p symmetry, which in this case would be the $2t_{1u}$ and $3t_{1u}$ orbitals. It is further assumed that the main oxygen K emission component originates in the t_{2u} and t_{1g} nonbonding 2p "lone-pairs." Peaks C and D in the L_{III} band and $K\beta$ in the K band would then be due to the $1e_g$, $1a_{1g}$, and $1t_{1u}$ levels which are associated primarily with oxygen 2s states. As can be seen in Figure 4, one of the really attractive features of such an MO interpretation is that orbitals such as $1t_{2g}$, $2t_{2g}$, and $3e_g$ which consist of admixed 3d and 2p states contribute components to both the CrL_{III} and OK spectrum. Furthermore, the relative intensities of the peaks reflect the relative degrees of admixture which would be intuitively expected from the normal assumptions

made about the individual orbitals as being either strongly bonding or slightly bonding and as being localized primarily on either the metal ion or ligand. The MO assignments for all the peaks are summarized in Table II.

One of the more significant consequences of the peak assignments discussed above is brought to light by a closer examination of peaks B, b, and d in the CrL_{III} spectrum. Peak B actually consists of two components, B_1 and B_2 . It is suggested here that all four of these components, B_1 , B_2 , b, and d involve $2t_{2g}$ orbitals. This is a consequence of the two different but simultaneous kinds of bonding involving the 3d (t_{2g}) electrons. In the corundum structure, c-axis cation-cation pairs are formed, and strong t_{2g} - t_{2g} covalent bonding can occur between the cations (in this case, chromium) forming the pair (References 22, 25, and 26). The other type of bond is the t_{2g} - $p\pi$ (chromium-oxygen) bond. For these two types of bonding to be clearly observable in the L_{III} spectrum, the $2t_{2g}$ orbitals would be required to become non-degenerate and split apart considerably in energy. Some splitting will occur as a consequence of the trigonal field in the corundum structure. Also, the chromium atoms forming the c-axis pairs have the closest cation-cation distances in the structure (see Table I) and the t_{2g} orbitals associated with the covalent bonding in this pair could exhibit a rather large bonding-antibonding splitting (References 22 and 25). The antiferromagnetic ordering could further contribute to the splitting. Therefore, it is suggested that CrL_{III} components B_1 and d represent the bonding and antibonding set of the $2t_{2g}$ orbital associated with chromium-chromium covalent bond. These components are labeled $2t_{2g}^b(\text{M})$ and $2t_{2g}^a(\text{M})$ respectively (Figure 4) and are assumed to be single electron states. The $2t_{2g}^b(\text{M})$ orbital is occupied, the $2t_{2g}^a(\text{M})$ orbital is vacant. Components B_2 and b would then represent the occupied and vacant two-electron states associated with the $3d$ - $2p\pi$ bond. They are labeled $2t_{2g}(\text{X})$ and $2t_{2g}^*(\text{X})$ in Figure 4.

The three outermost electrons in Cr_2O_3 are therefore involved in two distinct bonding mechanisms. One of the electrons is localized in a metal-metal covalent bond and the other two are associated with the

metal-oxygen π bond. Whether or not this latter orbital has a true energy gap between the occupied and vacant states is not clear from the x-ray spectra but the Fermi energy is assumed to be in this region. There is no obvious evidence of a collectivized orbital.

The above interpretation is further supported by the fact that since components B_1 and d represent the metal-metal covalent bond, they should consist of pure 3d character (more or less) and therefore should not contribute to either the CrK or OK spectra. As can be seen in Figure 4 there are indeed no components in either of the K spectra corresponding to the energy positions of B_1 and d. On the other hand since components B_2 and b in the L_{III} spectrum are interpreted as being due to the 3d-2p π bond, they should also contribute something to the oxygen K spectrum and perhaps also to the Cr K spectrum. It is seen in Figure 4 that these contributions do actually occur, as evidenced by peaks D and b in both the O K and Cr K spectra. These spectral relations are also evident in Table VI.

Actually, the above interpretation of peaks B, b, and d in the L_{III} spectrum is not based solely on the results obtained for Cr_2O_3 . Much consideration was also given to the TiL_{III} spectrum from Ti_2O_3 and the VL_{III} spectrum from V_2O_3 which have been shown previously (References 2, 3, and 4). It is an experimental fact that the relative intensity of emission component B and also absorption component b in these oxides is directly proportional to the number of 3d electrons while the intensities of components F, A, and G remain virtually unchanged with respect to each other. It must be concluded, therefore, that components B and b are associated with the partially occupied $2t_{2g}$ orbital and that components F, A, and G are associated with orbitals which are filled in all cases (see Table II).

The CrK band shown in Figure 4 has been interpreted by Menshikov and Nemnonov (Reference 24) in terms of two different types of d electrons but their interpretation is not in agreement with the one presented here. They concluded that the $K\beta'_5$ peak was associated with the collectivized (conduction) d electrons, the $K\beta_5$ peak with the localized d electrons,

and the $K\beta''$ peak as due to a crossover transition of the oxygen valence electrons to the chromium K level. According to the MO model of Figure 4, however, all three of the $K\beta$ peaks are seen to be associated with localized orbitals consisting partially of chromium 4p character. Peak $K\beta'_5$ arises from the 4p-2p π bond, peak $K\beta_5$ from the 4p-2p σ bond, and peak $K\beta''$ from the 4p-2s bond. This interpretation is more in accord with the dipole selection rules than that offered by Menshikov and Nemnonov. It serves, however, as a good example of the advantage gained in using the combined K and L spectra for structure determinations instead of relying on one spectrum alone.

Adler and Brooks (Reference 16) have postulated that the d bands in transition metal oxides, such as Ti_2O_3 and V_2O_3 , are extremely narrow, being on the order of a few tenths of an eV in width. From their arguments one would also expect the narrow band model to apply to Cr_2O_3 . In fact if anything, the d bands in Cr_2O_3 would likely be even narrower than in the corresponding titanium and vanadium oxides because when moving across the 3d series the d orbitals are contracted by the increased nuclear charge and nearest-neighbor overlap would not be as great (Reference 26). The x-ray band spectra, however, do not appear to support the narrow-band model. In the case of Cr_2O_3 , the CrL_{III} emission band has been resolved into 5 components and the L_{III} absorption into 3 components as shown in Figure 4. The measured half-widths and relative integrated intensities of these components are listed in Table VI. Before trying to relate the measured component widths to the actual electron orbital widths, we must first correct them for various broadening effects. The two primary effects to consider here are the width of the instrumental window and the width of the core level. For the experimental arrangement used to obtain the CrL_{III} band, the spectrometer window width is approximately 0.8eV. The chromium L_{III} level is believed to have a width of about 0.4eV (Reference 27). This means that the experimental probe has a total full width at half maximum of about 0.9eV. Molecular vibrations and spin-orbit coupling may also cause some level broadening but will probably amount to no more than a few tenths of an eV. As can be seen in Table VI, the uncorrected component widths are considerably

larger than the sum of the broadening distortions just mentioned. The B_1 and d components, for instance, which are associated with the d orbitals of the cation-cation bond have a measured half-width of 3.0eV. Assuming a conservatively large correction of 1.3eV, there is still at least a 1.7eV width which remains. Similarly, the d orbitals of the cation-anion bond (components B_2 and b) would have a corrected half width of about 1eV. While these values contain some uncertainties, it is nevertheless apparent that the d orbitals in Cr_2O_3 are considerably broader than is proposed in the Adler-Brooks model (Reference 16). This is also the case in the x-ray band spectra of the titanium and vanadium oxides shown previously (References 2,3,4, and 6). Some recent photoemission studies on TiO_2 and VO_2 by Derbenwick also fail to support the narrow d band model (Reference 28).

The components of the oxygen K spectrum tend to be narrower than those of the CrL_{III} spectrum as indicated in Table VI. This is mainly due to the fact that both the spectrometer window width (0.5eV) and inner level width (0.2eV) are smaller for the oxygen spectrum. All of the individual molecular orbitals in Cr_2O_3 appear to have half widths on the order of 1 to 2eV. Some solid-state broadening should be expected due to electron interactions between atoms in neighboring octahedra. Also, the distortion from ideal octahedral symmetry may cause unresolved splitting of degenerate orbitals which would make levels appear broadened.

If the method of unfolding the spectra, especially the CrL_{III} band, is accepted as being reasonably correct, then the relative intensities of the components can be used to provide a general indication of the amount of 3d character in the e_g and t_{2g} valence orbitals. The results are given in Table VII. In determining the values in the last column of the table, it was first assumed that the single-electron $2t_{2g}$ orbitals associated with the chromium-chromium covalent bond (components B_1 and d) represented 100% d character. These components were assigned an arbitrary intensity value of 100 and the other component intensities then scaled on a relative basis to them. The relative intensity values were then divided by the number of electron states appropriate to the orbital. It is difficult to

assess the accuracy of the results since they depend primarily on the unfolding procedure. It must first of all be assumed that the transition probability remains constant throughout the band. In addition, there are certain reservations about relating the intensities of absorption components on the same basis as emission components. Nevertheless, the results given in Table VII are interesting, in that they confirm, in a general quantitative way, the expected degree of cation and anion contributions to the various t_{2g} and e_g orbitals. The bonding orbitals ($2e_g$ and $1t_{2g}$) are seen to be strongly polarized toward the oxygen ions whereas the antibonding orbitals ($3e_g$ and $2t_{2g}$) are polarized toward the chromium ions. According to the intensity values given in Table VII, there are 3.5d electrons in the occupied orbitals of Cr_2O_3 . In principal, this same technique could be applied to the K bands for determining the relative percentages of 2p and 4p character in the appropriate orbitals. In fact, if the relative intensities of all components in the K and L_{III} spectra were known, the relative contribution of all the atomic orbitals to each of the valence molecular orbitals could be empirically determined. For the particular case of Cr_2O_3 , however, not enough is known about the various parameters involved in the CrK band measurement (Reference 24) to attempt a meaningful unfolding of the spectrum. The authors' spectrometer does not have the necessary resolution at this short wavelength (2.1\AA) to permit an accurate K band measurement.

According to the MO interpretation which has just been suggested, all of the individual molecular orbitals of Cr_2O_3 can be empirically placed on a relative energy scale as in Figure 4. The energy values of each x-ray component are listed in Tables III and V. This data could be placed on an absolute scale if accurate binding energies were obtained for the inner subshells by electron spectroscopy measurements. This author is unaware of any such work done for Cr_2O_3 but the usefulness of the measurements has been demonstrated by Anderman and Whitehead (Reference 15) for some sulfur and chlorine compounds.

There is one other piece of experimental evidence that can be used to gauge the correctness of the empirical MO structure of Figure 4. That evidence is found in the optical absorption spectrum of α -Cr₂O₃ measured by Neuhaus (Reference 29). The first prominent peak in that spectrum is at 2.1eV and is believed to be a measure of Δ , the ligand field-splitting parameter. In Cr₂O₃, Δ would correspond to the energy separation between the $2t_{2g}^*$ and $3e_g$ orbitals. Figure 4, however, shows both of these orbitals (absorption peaks b and c) to be vacant, and so no electrons are normally available to give rise to an optical transition between them. Also (from Figure 4 and Table III) note that the energy separation between the highest occupied orbital (B_2) and the lowest vacant orbital (b), both of which have $2t_{2g}$ symmetry, is 2.2eV. This is in good agreement with the optical value, and apparently it is this separation and not Δ that the optical absorption spectrum is measuring.

It is also of some interest to note that the MO structure of Figure 4 indicates that the oxygen 2s levels are involved in the bonding in Cr₂O₃. The presence of peaks C and D in the L_{III} band and peak $K\beta$ in the K band cannot be readily accounted for unless there is assumed to be slight interaction between the O2s level and the Cr 3d, 4s, and 4p levels.

From the preceding discussions we are now in a position to list several points in support of the MO interpretation which has been suggested for the x-ray band spectra of Cr₂O₃. The facts of note are:

- 1.) Individual x-ray spectra. The main peaks in each spectrum follow the expected selection rules, i.e., main peaks in the L band arise only from orbitals having considerable d or s character; main peaks in the K band arise only from orbitals having considerable p character.
- 2.) Combined x-ray spectra. Orbitals which consist of admixed chromium 3d and oxygen 2p symmetries ($1e$, $2e$, $2t_{2g}$. . .) contribute to both the chromium L and oxygen K bands. Orbitals which are virtually atomic in character (t_{2u} , cation pair t_{2g}) contribute only to the appropriate spectrum of the element involved.

- 3.) The intensities of CrL_{III} spectral components associated with the bonding and antibonding t_{2g} and e_g orbitals show the expected relative contributions of 3d and 2p symmetries.
- 4.) The separation between the highest occupied and lowest vacant orbitals as measured by the x-ray spectra is in good agreement with that measured by the optical absorption spectrum.
- 5.) There are no "left-over" components in the unfolded spectra. Each component can be logically assigned to a specific molecular orbital.

In addition to the above points, it is found that the empirically deduced energy positions of the individual orbitals in Cr_2O_3 are in reasonable agreement with calculations made for other octahedrally coordinated chromium complexes, e.g., CrF_6^{-3} (Reference 30). The ordering of the orbitals is slightly different in the empirical structure but the relative energy ranges in which they occur show tolerable agreement. Further support for the MO method will be found in the following sections on tetrahedral chromium-oxygen compounds.

C. CrO_4^{-2}

In the CrO_4^{-2} ion the chromium atom is surrounded by a regular tetrahedral arrangement of oxygen atoms. This tetrahedral field will result in a different molecular orbital structure than that of octahedral Cr_2O_3 , as illustrated in Figure 3. Consequently, considerable differences should also be observed in the CrL_{III} , CrK, and OK x-ray band spectra.

In obtaining the x-ray bands, three different chromates were studied: Na_2CrO_4 , K_2CrO_4 , and PbCrO_4 . As expected, they each yielded virtually identical spectra. Both the emission and absorption spectra shown in this report are from Na_2CrO_4 .

The CrL_{III} x-ray spectrum from CrO_4^{-2} is shown in Figure 1. Notice that it is indeed quite different in appearance from the Cr_2O_3 spectrum. The oxygen K spectrum is shown in Figure 2. These two spectra are then combined with Best's CrK band (Reference 8) in Figure 5. The object of Figure 5 is to empirically deduce the CrO_4^{-2} MO structure in a manner similar to that of the previous section for Cr_2O_3 . A general schematic of the type of MO structure we might expect to obtain is illustrated in Figure 3. Lining up each of the spectra in Figure 5 on a common energy scale is accomplished by positioning the absorption maxima directly in line with each other. The reasoning behind this will become apparent shortly. The zero of energy is arbitrarily placed at the L_{III} absorption edge, which is assumed to be the position of the Fermi energy.

As with Cr_2O_3 , it is again assumed that the dipole selection rules dictate the main peak assignments in the CrO_4^{-2} spectra. The CrL_{III} band should therefore reflect primarily the distribution of 3d states and we will begin by assigning emission component A in Figure 5 as due to a transition from a filled molecular orbital made up of mostly 3d symmetry. From the schematic diagram of Figure 3, we find that the $1e$ level satisfies this condition. Similarly, the strongest peak in the CrK emission band ($K\beta_{2,5}$) should arise from a filled orbital consisting mostly of p symmetry, which is identified here as the $2t_2$ orbital. In the CrL_{III} and OK absorption spectra the first two maxima are assumed to represent the two lowest empty MO's which are the $2e$ and $4t_2$. According to electron spin resonance measurements, the $2e$ is below $4t_2$ (Reference 31) and the x-ray results support this. The CrK absorption spectrum shows only one distinct maximum in this region and is assumed to be associated with the $4t_2$ level. The $2e$ level should not contribute significantly to the K spectrum because it consists of mostly 3d symmetry. This is why the absorption peaks c were lined up at the same energy position and labeled $4t_2$. Having now placed the $1e$, $2e$, $2t_2$, and $4t_2$ orbitals on the energy scale, the only one remaining which could be reasonably expected to contribute to peak F in the CrL_{III} band is $3t_2$. It is further assumed that the primary oxygen K emission component is due to transitions from the t_1 nonbonding 2p orbitals. The other assignments

follow logically as explained previously for the VO_4^{-3} structure (Reference 6). The energy positions and MO assignments of each of the components are summarized in Tables II, III, IV, and V. As a result of the above interpretation, all of the CrO_4^{-2} valence molecular orbitals are accounted for.

Best has also interpreted his CrK spectrum from CrO_4^{-2} on the basis of an MO model (Reference 8). It is basically the same as the interpretation offered here except for one point. Best concludes that the $K\beta_{2,5}$ peak arises from transitions from the $3t_2$ orbitals instead of the $2t_2$ orbital as suggested in Figure 5. If that were correct, then component F in the L_{III} band could not be accounted for. This is a further example of the advantage of using the combined K and L bands instead of depending on any one spectrum by itself.

The MO structure of CrO_4^{-2} as shown in Figure 5 has no partially occupied orbital as Cr_2O_3 does (Figure 3). In tetrahedral compounds, Cr has a +6 valence state, so that all the bonding orbitals are exactly filled and all the antibonding orbitals completely empty. This is reflected in the CrL_{III} emission bands of Figure 1. There is a peak labeled B in the Cr_2O_3 spectrum but not in the spectra of the three tetrahedral compounds. The presence of peak B in a CrL_{III} band from a compound always signifies that the lowest antibonding orbitals is partially occupied.

Now that we have shown how the MO structure of CrO_4^{-2} can be determined empirically from x-ray spectra, it is of interest to see how this structure compares with some experimental data and theoretical calculations made by others. The CrO_4^{-2} optical absorption spectrum has two primary peaks at 3.32 and 4.54eV (Reference 32). These peaks have been interpreted in at least four different ways. In 1952, Wolfsberg and Helmholtz (Reference 33) calculated an MO structure for CrO_4^{-2} , in which the highest filled orbital was t_1 and the lowest empty orbital was $4t_2$. On this basis, they interpreted the optical spectrum as indicated in Table VIII, column 2. Later, Ballhausen and Liehr (Reference 34)

disagreed with the Wolfsberg-Helmholz scheme, suggesting that the lowest empty orbital was $2e$ instead of $4t_2$. They then reinterpreted the optical spectrum as being due to the transitions listed in column 3 of Table VIII. That the lowest empty orbital is indeed $2e$ was further supported by Carrington and Schonland's ESR measurements. Another MO calculation was made by Viste and Gray (Reference 35) using certain simplifying assumptions which resulted in their calling the structure "pseudo" CrO_4^{-2} . They then interpreted the optical spectrum in yet a third way as indicated in column 4 of Table VIII. Oleari et al. (Reference 36) performed a self-consistent MO calculation for CrO_4^{-2} and interpreted the optical spectrum in terms of multiple transitions for each peak as indicated in column 5 of Table VIII. They justified their multiple assignments by pointing out that the absorption bands are quite broad and that the second band actually has a shoulder. Surprisingly, the x-ray results do not agree completely with any of these previous interpretations. The problem stems from the assumed MO structure in the vicinity of the Fermi energy. All of the previous workers assumed that the highest filled orbital was the nonbonding t_1 . The x-ray spectra in Figure 5 indicate that this is not correct and that the highest filled orbital is actually $3t_2$. This x-ray deduced structure is compared with the calculated Viste-Gray and Oleari et al. structures in Figure 6. All three structures are placed on the same relative scale by arbitrarily placing the zero energy point at the t_1 nonbonding level. The Wolfsberg-Helmholz calculation is not included in the figure because it doesn't come even close to agreeing with the x-ray results and is, at any rate, generally considered to be incorrect. As can be seen in Figure 6, the x-ray results are far from agreement with the Oleari et al. calculations despite the fact that they are supposedly self-consistent. They made two calculations, for chromium charge numbers of 0 and +1. The diagram shown in Figure 6 is for the +1 charge. The 0 charge diagram shows even less agreement. A rather odd feature of the results of Oleari et al. is the extremely large energy separation ($\sim 9\text{eV}$) between the highest filled and lowest empty orbitals. Much better agreement is found in comparing the x-ray results with the Viste-Gray calculations which were considered very rough to begin with (Reference 35). Perhaps the disagreements should not be very

surprising in light of Fensky and Sweeny's conclusion (Reference 37), that the final outcome of the calculations depends very strongly on the initial assumptions made in determining symmetry characters of hybridized orbitals.

The x-ray deduced MO structure of CrO_4^{-2} is further supported by a different interpretation of the optical absorption spectrum. On the basis of the orbital positions determined in Figure 5, the optical peaks at 3.32 and 4.54eV can be assigned to the transitions $t_1 \rightarrow 2e$ and $3t_2 \rightarrow 4t_2$, respectively. It is emphasized that these orbital energy differences agree exactly with the optical peak positions, which is often not the case in the other work referred to. According to Ballhausen and Liehr's interpretation, e.g., the $2e$ and $4t_2$ orbitals would be separated by only 1.2eV. This is certainly too small as indicated by the CrL_{III} x-ray absorption spectrum, the OK absorption spectrum, and the optical spectra of other, similar compounds (References 35 and 38). This energy separation is also known as Δ , the ligand field-splitting parameter. The x-ray spectra shown here indicate a Δ value of 2.3eV. The x-ray results also indicate that each of the two absorption peaks has a unique transition assignment and that multiple assignments such as suggested by Oleari et al. (Reference 36) are incorrect. Table VIII summarizes the CrO_4^{-2} situation.

Oleari et al. (Reference 36) have also stated that during a charge-transfer excitation the antibonding MO energy separation ($4t_2-2e$) changes, and that it is therefore impossible to derive from experimental data (specifically optical absorption) an empirical evaluation of the $4t_2-2e$ energy separation. This seems questionable and most certainly does not hold true for the experimental x-ray data. As seen in Figure 5, both the CrL_{III} and oxygen K absorption spectra give directly the $4t_2-2e$ energy separation as reflected in peaks b and c. If the $2e$ and $4t_2$ orbitals are considered to be localized primarily on the Cr atom, then the oxygen K absorption could be thought of as arising from a charge-transfer excitation, while the CrL_{III} absorption represents an intra-atomic transition. Both spectra give the same energy separation for peaks b and

c (Figure 5), and hence the same $4t_2-2e$ energy separation. These two orbitals are also involved in optical absorption transitions and the agreement between the optical and x-ray data was discussed in the preceding paragraph.

It may have been noticed by the reader that component A in the oxygen K emission band of Figure 5 has not been assigned to any particular orbital. This is due to the fact that component A does not appear to have anything to do with the CrO_4^{-2} ion. In the chromates, the oxygens are involved in bonding to two different metal ions. In Na_2CrO_4 , for instance, there are Cr-O and Na-O bonds, the latter probably being highly ionic. After observing the oxygen K band from several different chromates it appears that component A is associated with the oxygen bond to the other metal ion, although it is much more intense than would normally be expected. The reason for this is not clear at present.

Viste and Gray (Reference 35) have emphasized the importance of including the oxygen 2s level in any MO calculation of the valence orbitals in tetrahedral oxyanions. The x-ray band spectra shown here support their point because peaks C and D in the L_{III} spectrum and $K\beta''$ in the K spectrum could not be accounted for without assuming 2s participation in the bonding. This was also the case in the VO_4^{-3} spectra (Reference 6). Furthermore, in Figure 6 it is obvious that the x-ray MO structure is in much closer agreement with the calculations of Viste and Gray (who included 2s participation) than it is with the calculations of Oleari et al. (who did not).

There is no indication from the x-ray spectra of a significant energy gap between the top of the highest filled and the bottom of the lowest empty orbitals in CrO_4^{-2} . Since these orbitals are highly localized on the molecule, a gap is not necessary to explain the lack of electrical conductivity. If a gap is present, it would probably not be detectable by the x-ray spectra anyway because of the presence of multiple ionization satellite structure at the emission edge which would completely mask the true position of the edge. The only way this problem could be

overcome would be to obtain the L_{III} band at threshold excitation (Reference 39) which is too difficult to be practical in this case.

The CrL_{III} band in Figure 5 was resolved into the Gaussian components by the method described in section IIIA. Since there is believed to be no significant interaction between neighboring tetrahedral units, in CrO_4^{-2} (Reference 8), the individual orbitals should not be broadened to quite the extent observed in Cr_2O_3 . With the exception of component G the CrO_4^{-2} orbitals do indeed appear to be somewhat narrower. The width of component G is probably greatly exaggerated in Figure 5 because an attempt was made to make the unfolds match the low energy tail of the L_{III} band without introducing another component. Extended tailing due to Auger transitions, certain types of excitation states, etc. (Reference 14) could therefore make component G (and to a lesser extent, component A) appear much broader than it really is. This is also true for components G and E in the Cr_2O_3 spectrum in Figure 4.

D. CrO_3

In CrO_3 , the oxygen atoms form distorted tetrahedra around the Cr atoms (Reference 40). As indicated in Table I, both the Cr-O and Cr-Cr interatomic distances are considerably different than in CrO_4^{-2} . Even though the CrO_3 tetrahedra are distorted, the soft x-ray band spectra would be expected to be similar in appearance to the CrO_4^{-2} spectra. To a large degree this similarity is actually observed as seen in Figures 1 and 2. The specific spectral differences which occur are attributed to the symmetry distortion, as explained below.

The CrL_{III} and OK spectra from CrO_3 are displayed on the same energy scale in Figure 7. These spectra are aligned with each other by the method described in the previous section concerning Figure 5. No CrK spectrum is shown because apparently no one has ever published it. The author's spectrometer does not have sufficient resolution at 2\AA to obtain

a detailed K band which would be needed here. Without the CrK band, unfortunately, the complete MO structure of CrO_3 cannot be deduced. Nevertheless, considerable information is still present in the combined CrL_{III} and OK spectra of Figure 7. The unfolding of the spectra into individual components follows the method described in section IIIA. In making assignments for the spectral components, the same MO term symbols are used for CrO_3 as for a regular tetrahedral structure. This is not strictly permissible because the distorted symmetry will result in a splitting of the triply degenerate orbitals into a singlet and a doublet ($e+a_1$). It is very convenient, however, to retain the original term symbols for making comparisons of the CrO_3 spectra with what was previously shown for CrO_4^{-2} . In many cases, the symmetry distortion is reflected in the spectra only as a band broadening anyway.

The CrL_{III} emission band is essentially the same as obtained from CrO_4^{-2} except that the components are broadened as seen in Figure 7. Peaks F, A, G, C, and D are therefore interpreted in the same way (Table II). In the oxygen K emission band component B is again assigned as arising from the t_1 nonbonding orbital. Components C and G correspond to the A and G components of the L_{III} band. The big difference in CrO_3 as compared to CrO_4^{-2} occurs in the absorption spectra. The most noticeable change is the appearance of a new L_{III} component, labeled g. It is suggested that component g is associated with nonbonding chromium e orbitals since the tetrahedral distortion is such that some of the e orbitals could not form bonds with the oxygen 2p orbitals (Reference 40). This interpretation is reinforced by the fact that there is no corresponding component observed in the oxygen K spectrum. Another noticeable aspect of the absorption spectra is that peak c has apparently split into two easily separated components, c_1 and c_2 . This splitting occurs in both the CrL_{III} and OK spectra and may indicate the a_1 and e components of the original $4t_2$ orbital. The energy positions of each spectral component are listed in Tables III and IV.

It would be helpful to have some other experimental data for CrO_3 with which to compare the x-ray results but none could be found.

Apparently the optical absorption spectrum has not been published and no electronic structure calculations have been made. The MO interpretation of the x-ray band spectra, however, does appear to be supported by what is known about CrO_3 . It is concluded that the empirically deduced MO structure is similar to that obtained for CrO_4^{-2} (Figure 5) except that the tetrahedral distortion has caused some obvious splitting of the $4t_2$ orbital and has also caused the formation of nonbonding chromium e orbitals.

E. $\text{Cr}_2\text{O}_7^{-2}$

The ammonium, sodium, and potassium dichromates crystallize in a monoclinic structure in which the oxygen atoms form extremely distorted tetrahedra around the chromium atoms (Reference 41). As indicated in Table I, the Cr-O bonding distances (and angles) vary considerably. Such extreme distortion may cause a splitting of all degenerate orbitals although no calculations have been made on this sort of structure. As in the case of CrO_3 , the regular tetrahedral term symbols are used for the sake of convenience in interpreting the x-ray band spectra.

The CrL_{III} spectrum from $\text{K}_2\text{Cr}_2\text{O}_7$ is shown in Figure 1. The sodium and ammonium salts give spectra virtually identical to this. As can be seen, this spectrum looks very much like that obtained from CrO_3 and CrO_4^{-2} . The oxygen K spectrum is shown in Figure 2, and is matched to the CrL_{III} spectrum in Figure 8. No Cr K spectrum is available for comparison. Due to the extreme symmetry distortion and lack of other experimental data, no clearcut arguments can be offered in support of the empirical MO structure for $\text{Cr}_2\text{O}_7^{-2}$ shown in Figure 8. Since the spectra have the same general appearance as shown earlier for CrO_4^{-2} and CrO_3 , the only reasonable approach is to make an analogous interpretation. Energy positions of each of the components and their assignments are listed in Tables II, III, IV, and V.

SECTION IV

SUMMARY AND CONCLUSIONS

It has been shown that a complete valence molecular orbital structure can be empirically deduced for chromium-oxygen compounds by combining the information present in the CrL_{III} , CrK , and OK x-ray band spectra. MO assignments are made on the basis of the energy positions and relative intensities of the unfolded x-ray components in conjunction with other experimental data and theoretical calculations. All of the emission and absorption components are seen to be logically explained in terms of bonding, antibonding, and nonbonding molecular orbitals.

In Cr_2O_3 , the L_{III} x-ray spectrum indicates that the three outermost electrons have t_{2g} symmetry and are involved in two distinct bonding mechanisms. One of these electrons is localized in a metal-metal covalent bond (c-axis pairing) and the other two are associated with a $\text{Cr-O } \pi$ bond. There is no obvious evidence of a collectivized d orbital. After corrections for broadening effects, the predominantly 3d orbitals of Cr_2O_3 are found to have a half-width on the order of 1 to 1.5 eV. The narrow d-band model of Adler and Brooks (Reference 16) is therefore not supported. Relative intensities of the CrL_{III} spectral components can be used to indicate the approximate amount of 3d contribution to each of the bonding and antibonding e_g and t_{2g} orbitals in Cr_2O_3 (Table VII). The x-ray absorption spectra indicate that Δ , the ligand field-splitting parameter, is 2.1 eV in Cr_2O_3 but that the optical absorption spectrum does not measure Δ as is often assumed. It is probably the separation between the highest occupied and lowest empty orbitals, both of which have t_{2g} symmetry in Cr_2O_3 , that the optical spectrum is measuring.

The empirically deduced MO structure of CrO_4^{-2} is not in good agreement with previous calculations (Figure 6). At least four different interpretations have been previously suggested for the optical absorption spectrum of CrO_4^{-2} but none of them are consistent with the x-ray results. A different interpretation therefore, is offered here (Table VIII).

It is concluded that, contrary to previous assumptions, the highest filled orbital in CrO_4^{-2} is $3t_2$ instead of t_1 . The x-ray absorption spectra support ESR measurements (Reference 31) in indicating that the lowest empty orbital is $2e$. It is determined that Δ is 2.3eV.

In going from CrO_4^{-2} to CrO_3 to $\text{Cr}_2\text{O}_7^{-2}$, the tetrahedral symmetry becomes increasingly distorted. This is mirrored in the x-ray band spectra as a broadening and splitting of certain orbitals and by the formation of nonbonding chromium orbitals in CrO_3 and $\text{Cr}_2\text{O}_7^{-2}$. These spectral variations are expected on the basis of MO theory and provide additional support for interpreting the spectra in MO terms.

The presence of peaks C and D in the CrL_{III} band and peak K β'' in the the CrK band show that the oxygen 2s orbitals are involved in the bonding in each of the compounds discussed here.

To obtain a complete valence molecular-orbital diagram of transition metal compounds, it is necessary to use the combined K and L x-ray bands of the metal ion and anion as in Figures 4 and 5. No one spectrum by itself is sufficient. This is because the valence orbitals contain a strong admixture of p, d, and s symmetries and the dipole selection rules prevent certain transitions from occurring in each x-ray state.

Although the molecular orbital structures determined in this report are strongly empirical in nature they nevertheless point out the great value of x-ray valence band spectra in studying the electronic structure and chemical bonding in solids. Molecular orbital assignments can be made quite confidently for the various spectral components from simple considerations of peak positions and relative intensities in conjunction with the usual dipole selection rules. It is always helpful, of course, to have theoretical calculations and other types of experimental data at hand for comparison purposes. The great advantage of x-ray spectra over other experimental techniques is evident in both their simplicity and completeness. The combination of emission and absorption spectra makes it possible to locate both occupied and vacant orbitals within 20eV or so of the Fermi energy. In addition, the relative contributions of the

various atomic orbitals to each molecular orbital plus the energy width of each molecular orbital can be empirically determined from good, reliable x-ray data. Also, the atomic character of the inner vacancy considerably simplifies the problem of unambiguously assigning an electron transition to each spectral component. This overall simplicity, completeness, and flexibility cannot even be approached by any other single experimental technique. The real beauty of the MO interpretation as illustrated in Figures 4 and 5 is that it ties together very effectively the various cation and anion emission and absorption spectra with the chemical interactions which must occur between anion and cation in forming a compound. Strong relationships are seen between the x-ray spectra and various solid-state phenomena such as coordination symmetry, bonding distances, valence state, bonding character, and many of the resulting physical properties. Certainly more complete work needs to be done in certain areas, particularly in persuading theoreticians to do more careful MO structure calculations which can be directly compared with the experimental data that can now be obtained. Even with the present state of affairs, however, it is quite apparent that soft x-ray band spectroscopy is an extremely powerful tool for probing the electronic structure of compounds.

REFERENCES

1. ADLER, D., Rev. Mod. Phys. 40, 714 (1968).
2. FISCHER, D.W., and BAUN, W.L., J. Appl. Phys. 39, 4757 (1968).
3. FISCHER, D.W., J. Appl. Phys. 40, 4151 (1969).
4. FISCHER, D.W., J. Appl. Phys. 41 3561 (1970).
5. FISCHER, D.W., J. Appl. Phys. 41, 3922 (1970).
6. FISCHER, D.W., Applied Spectroscopy, 25, 263 (1971).
7. DODD, C.G., and GLEN, G.L., J. Appl. Phys. 39, 5377 (1968).
8. BEST, P.E., J. Chem. Phys. 44, 3248 (1966).
9. BEST, P.E., J. Chem. Phys. 49, 2797 (1968).
10. SEKA, W., and HANSON, H.P., J. Chem. Phys. 50, 344 (1969).
11. MANNE, R., J. Chem. Phys. 52, 5733 (1970).
12. LAWRENCE, D.F., and URCH, D.S., Spectrochim. Acta B 25, 305 (1970).
13. URCH, D.S., J. Phys. Soc, C 3, 1275 (1970).
14. NAGEL, D.J., Advan. X-Ray Anal. 13, 182 (1970).
15. ANDERMAN, G., and WHITEHEAD, H.C., Advan. X-Ray Anal. 14, 453 (1971).
16. ADLER, D., and BROOKS, H., Phys. Rev. 155, 826 (1967).
17. BALLHAUSEN, C.J., and GRAY, H.B., Molecular Orbital Theory, W. A. Benjamin, Inc., New York (1964).
18. FIGGIS, B.N., Introduction to Ligand Fields, John Wiley & Sons, Inc., New York (1966).
19. JORGENSEN, C.K., Absorption Spectra and Chemical Bonding in Complexes, Pergamon Press, New York (1962).
20. NEWNHAM, R.E., and DEHAAN, Y.M., Z. Krist. 117, 235 (1962).
21. BROCKHOUSE, B.N., J. Chem. Phys. 21, 961 (1953).
22. ADLER, D., FEINLEIB, J., BROOKS, H., and PAUL, W., Phys. Rev. 155, 851 (1967).
23. NEBENZAHL, I., and WEGER, M., Phys. Rev. 184, 936 (1969).

24. MENSNIKOV, A.Z., and NEMNOV, S.A., Bull. Acad. Sci. U.S.S.R. (Phys. Ser.) 27, 402. (1963).
25. GOODENOUGH, J.B., Phys. Rev. 117, 1442 (1960).
26. MORIN, F.J., J. Appl. Phys. 32, 2195 (1961).
27. PARRATT, L. G., Rev. Mod. Phys. 31, 616 (1959).
28. DERBENWICK, G.F., Stanford Electronic Laboratories. Tech. Rept. 5220-2 (1970).
29. NEUHAUS, A., Z. Krist. 113, 195 (1960).
30. Reference 17, page 130.
31. CARRINGTON, A., and SCHONLAND, D.S., Mol. Phys. 3, 331 (1960).
32. CARRINGTON, A., and SYMONS, M.C.R., J. Chem. Soc. (London), 889 (1960).
33. WOLFSBERG, M., and HELMHOLZ, L., J. Chem. Phys. 20, 837 (1952).
34. BALLHAUSEN, C.J., and LIEHR, A.D., J. Mol. Spectr. 2, 342 (1958).
35. VISTE, A., and GRAY, H.B., Inorg. Chem. 3, 1113 (1964).
36. OLEARI, L., DEMICHELIS, G., and DISIRIO, L., Mol. Phys. 10, 111 (1965).
37. FENSKY, R.F., and SWEENEY, C. C., Inorg. Chem. 3, 1105 (1964).
38. CARRINGTON, A., and JORGENSEN, C. K., Mol. Phys. 4, 395 (1961).
39. LIEFELD, R.J., In Soft X-Ray Band Spectra (Edited by D.J. Fabian), pp. 133-149, Academic Press, New York (1968).
40. BYSTROM, A., and WILHELM, K., Acts Chem. Scand. 4, 1131 (1950).
41. WYCKOFF, R.W.G., Crystal Structures, Interscience Publishers, New York (1953).

TABLE I
INTERATOMIC DISTANCES IN SOME CHROMIUM-OXYGEN COMPOUNDS

Compound	Cr Co-Ord No.	Structure	Cr-O Distances (Å)	Shortest Cr-Cr Distance (Å)
Cr metal	8	B.C.C.		2.50
Cr ₂ O ₃ *	6	Rhombohedral	O ₁ , O ₂ , O ₃ = 2.02 O ₄ , O ₅ , O ₆ = 1.57	2.65
CrO ₃ **	4	Orthorhombic	O ₁ , O ₂ = 1.79 O ₃ , O ₄ = 1.81	3.32
Na ₂ CrO ₄ ***	4	Orthorhombic	O ₁ , O ₂ , O ₃ , O ₄ = 1.60	4.62
(NH ₄) ₂ Cr ₂ O ₇ ***	4	Monoclinic	O ₁ = 1.55 O ₂ = 1.57 O ₃ = 1.77 O ₄ = 1.91	3.22

* Reference 20

** Reference 40

*** Reference 41

TABLE II

SUGGESTED ELECTRONIC TRANSITIONS RESPONSIBLE FOR INTENSITY MAXIMA
OBSERVED IN CHROMIUM $L_{II,III}$ EMISSION AND ABSORPTION SPECTRA FROM COMPOUNDS

EMISSION SPECTRA			
Peak	Electron Transition Octahedral Site	Electron Transition Tetrahedral Site	
B	$2t_{2g} \rightarrow 2p_{3/2}$	not observed	} L_{III} components
F	$1t_{2g} \rightarrow 2p_{3/2}$	$3t_2 \rightarrow 2p_{3/2}$	
A	$2e_g \rightarrow 2p_{3/2}$	$1e \rightarrow 2p_{3/2}$	
G	$2a_{1g} \rightarrow 2p_{3/2}$	$2a_1 \rightarrow 2p_{3/2}$	
C	$1e_g \rightarrow 2p_{3/2}$	$1t_2 \rightarrow 2p_{3/2}$	
D	$1a_{1g} \rightarrow 2p_{3/2}$	$1a_1 \rightarrow 2p_{3/2}$	
T	$2t_{2g} \rightarrow 2p_{1/2}$	not observed	} L_{II} components
K	$1t_{2g} \rightarrow 2p_{1/2}$	$3t_2 \rightarrow 2p_{1/2}$	
H	$2e_g \rightarrow 2p_{1/2}$	$1e \rightarrow 2p_{1/2}$	
E	$1a_{1g}, 1e_g \rightarrow 2p_{1/2}$	-----	
ABSORPTION SPECTRA			
Peak	Electron Transition Octahedral Site	Electron Transition Tetrahedral Site	
a	L_{III} edge	L_{III} edge	} L_{III} components
b	$2p_{3/2} \rightarrow 2t_{2g}$	$2p_{3/2} \rightarrow 2e$	
c	$2p_{3/2} \rightarrow 3e_g$	$2p_{3/2} \rightarrow 4t_2$	
g	-----	$2p_{2/2} \rightarrow en$	
k	L_{II} edge	L_{II} edge	} L_{II} components
m	$2p_{1/2} \rightarrow 2t_{2g}$	$2p_{1/2} \rightarrow 2e$	
n	$2p_{1/2} \rightarrow 3e_g$	$2p_{1/2} \rightarrow 4t_2$	
f	exciton (?)	exciton (?)	

TABLE III
ENERGY POSITIONS OF PEAK MAXIMA IN CHROMIUM L_{II,III} EMISSION AND ABSORPTION SPECTRA
(ALL VALUES GIVEN IN eV WITH PROBABLE ERROR OF ± 0.2 eV.)

EMISSION SPECTRA										
Material	B	F	A	G	C	D	T	H	K	
Cr metal	571.5	-	-	-	-	-	580.8	-	-	-
Cr ₂ O ₃	[572.1] [573.8]	569.2	566.4	563.4	553.2	551.3	582.3	-	-	-
CrO ₃	-	574.7	571.5	569.3	558.0	553.8	-	580.8	584.0	
Na ₂ CrO ₄	-	575.7	572.5	569.3	558.9	554.6	-	581.6	584.7	
Na ₂ Cr ₂ O ₇	-	573.9	571.7	570.3	558.7	553.8	-	581.5	586.2	
ABSORPTION SPECTRA										
Material	f	a	b	c	d	g	k	m	n	
Cr metal	-	573.8	574.6	575.7	577.2	-	583.3	584.2	585.2	
Cr ₂ O ₃	572.9	575.0	576.0	578.1	580.5	-	584.0	584.9	586.9	
CrO ₃	572.1	-	577.1	[578.9] [580.4]	-	575.9	-	586.2	588.2	
Na ₂ CrO ₄	573.9	576.9	577.9	580.2	-	-	-	-	-	
Na ₂ Cr ₂ O ₇	572.9	-	577.7	579.7	-	575.9	-	586.5	588.9	

TABLE IV

SUGGESTED ELECTRONIC TRANSITIONS RESPONSIBLE FOR INTENSITY MAXIMA
OBSERVED IN CHROMIUM K AND OXYGEN K X-RAY SPECTRA FROM CHROMIUM-OXYGEN COMPOUNDS

Spectrum	Peak	Electron Transition Octahedral Site	Electron Transition Tetrahedral Site
Cr K Emission	$K\beta_{2,5}$ (or $K\beta_5$)	$2t_{1u} \rightarrow 1s$	$2t_2 \rightarrow 1s$
	$K\beta'_5$	$3t_{1u} \rightarrow 1s$	not observed
	$K\beta''$	$1t_{1u} \rightarrow 1s$	$1t_2 \rightarrow 1s$
Cr K Absorption	b	$1s \rightarrow 2t_{2g}$	not observed
	c	$1s \rightarrow 3e_g$	$1s \rightarrow 4t_2$
	d	$1s \rightarrow 3a_{1g}$	$1s \rightarrow 5a_1$
	e	$1s \rightarrow 4t_{1u}$	$1s \rightarrow 5t_2$
O K Emission	A	$1t_{2g} \rightarrow 1s$	---
	B	$t_{1g}, t_{2u} \rightarrow 1s$	$t_1 \rightarrow 1s$
	C	$2t_{1u} \rightarrow 1s$	$1e \rightarrow 1s$
	D	$2t_{2g} \rightarrow 1s$	---
O K Absorption	a	K edge	K edge
	b	$1s \rightarrow 2t_{2g}$	$1s \rightarrow 2e$
	c	$1s \rightarrow 3e_g$	$1s \rightarrow 4t_2$
	f	exciton (?)	exciton (?)

TABLE V
ENERGY POSITIONS OF PEAK MAXIMA IN OXYGEN K EMISSION AND ABSORPTION SPECTRA
(ALL VALUES GIVEN IN eV WITH PROBABLE ERROR OF ± 0.2 eV.)

Material	Emission			Absorption		
	A	B	C	D	f	c
Cr_2O_3	523.0	524.7	521.7	527.7	527.5	529.3
CrO_3	-	525.5	523.6	-	526.4	529.1
Na_2CrO_4	523.8	525.2	522.6	-	526.5	528.5
$\text{Na}_2\text{Cr}_2\text{O}_7$	523.9	525.5	522.6	-	526.3	528.6
						531.9
						[531.0] [532.4]
						530.9
						[530.1] [530.8]

TABLE VI

LINE WIDTHS AND RELATIVE INTENSITIES OF UNFOLDS IN Cr_2O_3 BAND SPECTRA
(THE VALUES HAVE NOT BEEN CORRECTED FOR SPECTROMETER WINDOW OR INTERNAL LEVEL WIDTH.)

Spectrum	Component	Assigned MO	$\text{Wl}/2(\text{eV})$	Relative Integrated Intensity (Emission)
CrL_{III} (GAUSSIAN) 3d character	B_1	$2t_{2g}^b$ (M)cation-cation	3.0	89
	B_2	$2t_{2g}^x$ (X)cation-anion	2.4	100
	F	$1t_{2g}$	3.3	62
	A	$2e_g$	3.4	60
	G	$2a_{1g}$	3.8	21
	b	$2t_{2g}^*$ (X)cation-anion	2.4	--
	c	$3e_g$	2.1	--
	d	$2t_{2g}^a$ (M)cation-cation	3.0	--
OK (LORENTZIAN) 2p character	B	t_{2u}	2.8	100
	A	$1t_{2g}$	1.6	21
	C	$2t_{1u}$	1.7	23
	D	$2t_{2g}^x$	1.8	5
	b	$2t_{2g}^*$ (X)	1.1	--
	c	$3e_g$	1.5	--

TABLE VII
RELATIVE PERCENTAGES OF 3d CHARACTER IN e_g AND t_{2g} VALENCE ORBITALS OF
 Cr_2O_3 AS DETERMINED FROM UNFOLDED CrL_{III} BAND SPECTRUM

Component	Number of Electron States(n)	Relative Integrated Intensity	I/n = % d Character
$B_1(2t_{2g} \text{ Cr-Cr})$	1	100	100
$B_2(2t_{2g} \text{ Cr-O})$	2	112	56
$F(1t_{2g})$	6	70	12
$A(2e_g)$	4	67	17
occupied states (total 3.5d elec- trons)			
$b(2t_{2g} \text{ Cr-O})$	2	176	88
$c(3e_g)$	4	205	51
$d(2t_{2g} \text{ Cr-Cr})$	1	100	100
vacant states			

TABLE VIII
ELECTRON TRANSITION ASSIGNMENTS FOR TWO PRINCIPLE MAXIMA IN OPTICAL ABSORPTION SPECTRUM OF CrO_4^{2-}

Peak Position ¹	Wolfsberg & Helmholz ²	Ballhausen & Liehr ³	Viste & Gray ⁴	Oleary et al. ⁵	This Work (x-ray)
3.32eV	$t_1 \rightarrow 4t_2$	$t_1 \rightarrow 2e$	$t_1 \rightarrow 2e$	$\left\{ \begin{array}{l} t_1 \rightarrow 4t_2 \\ t_1 \rightarrow 2e \end{array} \right\}$	$t_1 \rightarrow 2e(3.3\text{eV})$
4.54eV	$3t_2 \rightarrow 4t_2$	$t_1 \rightarrow 4t_2$	$3t_2 \rightarrow 2e$	$\begin{array}{l} 3t_2 \rightarrow 4t_2 \\ 3t_2 \rightarrow 2e \\ 3t_2 \rightarrow 3a_1 \end{array}$	$3t_2 \rightarrow 4t_2(4.5\text{eV})$
Highest occupied orbital	t_1	t_1	t_1	t_1	$3t_2$
Lowest vacant orbital	$4t_2$	$2e$	$2e$	$3a_1$	$2e$
$\Delta(\text{eV})$	1.6	1.2	3.1	0.5	2.3

- 1 Reference 32
- 2 Reference 33
- 3 Reference 34
- 4 Reference 35
- 5 Reference 36

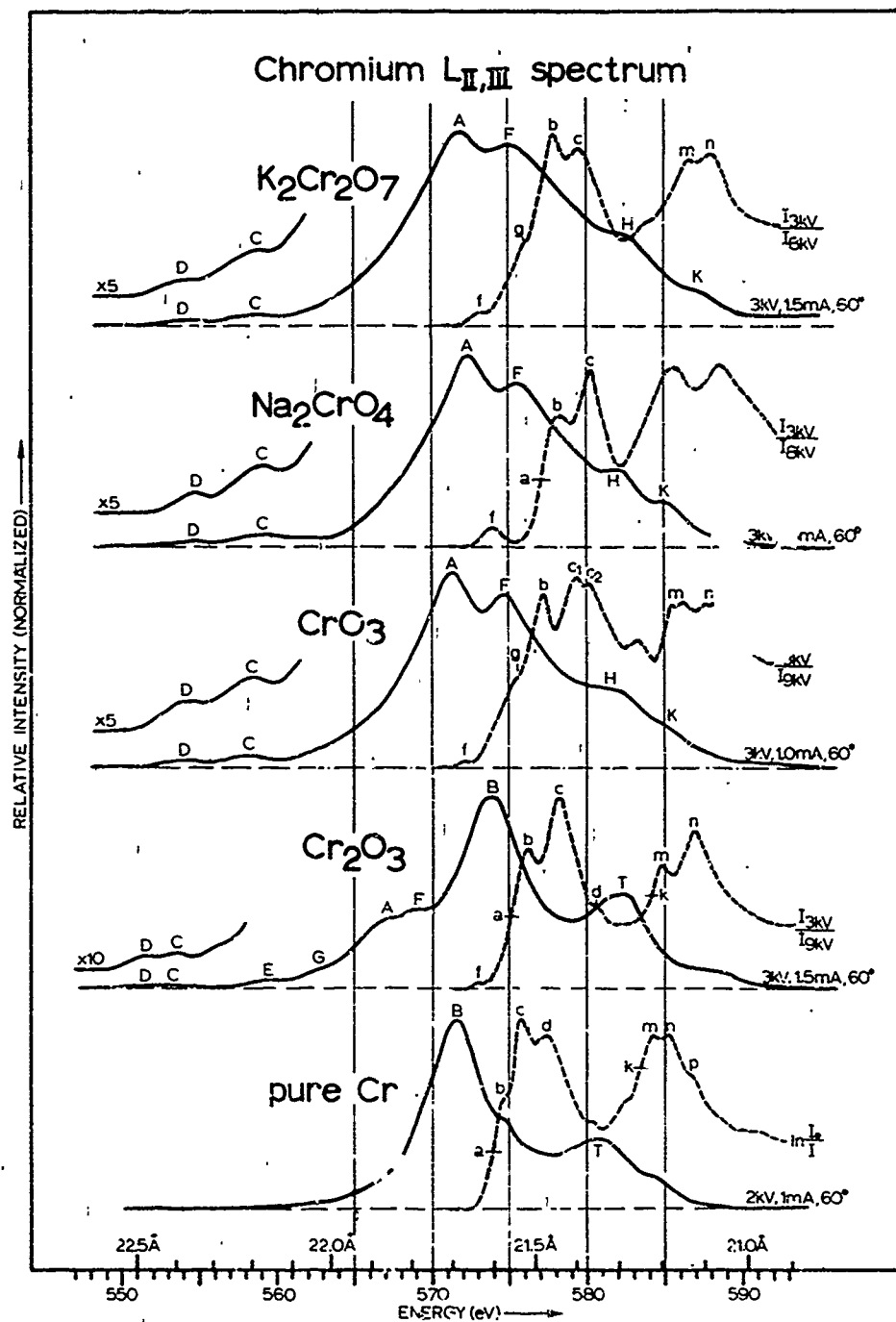


Figure 1. Uncorrected chromium $L_{II,III}$ emission and absorption spectra from pure element and compounds. Emission bands obtained under negligible self-absorption conditions. Absorption spectra from compounds are self-absorption replicas. All spectra normalized to same height for comparison purposes.

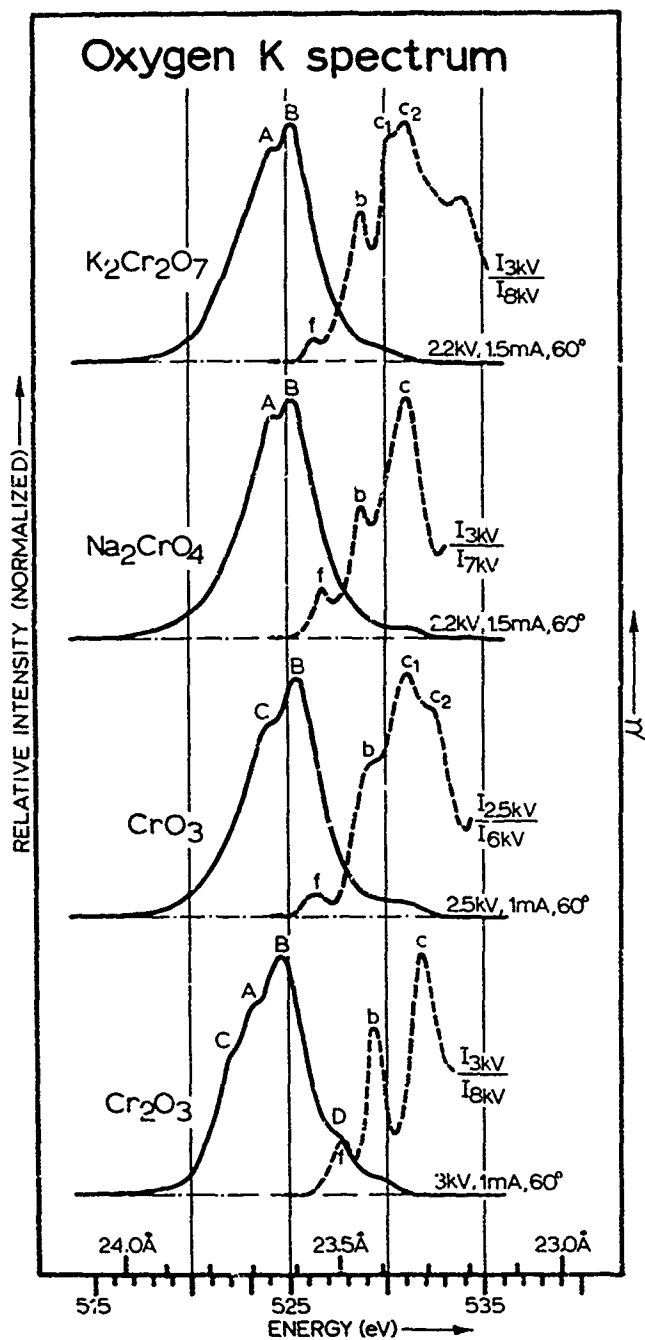


Figure 2. Uncorrected oxygen K emission and absorption spectra. Emission bands obtained under negligible self-absorption conditions. Absorption spectra are self-absorption replicas. All spectra normalized to same height for comparison purposes.

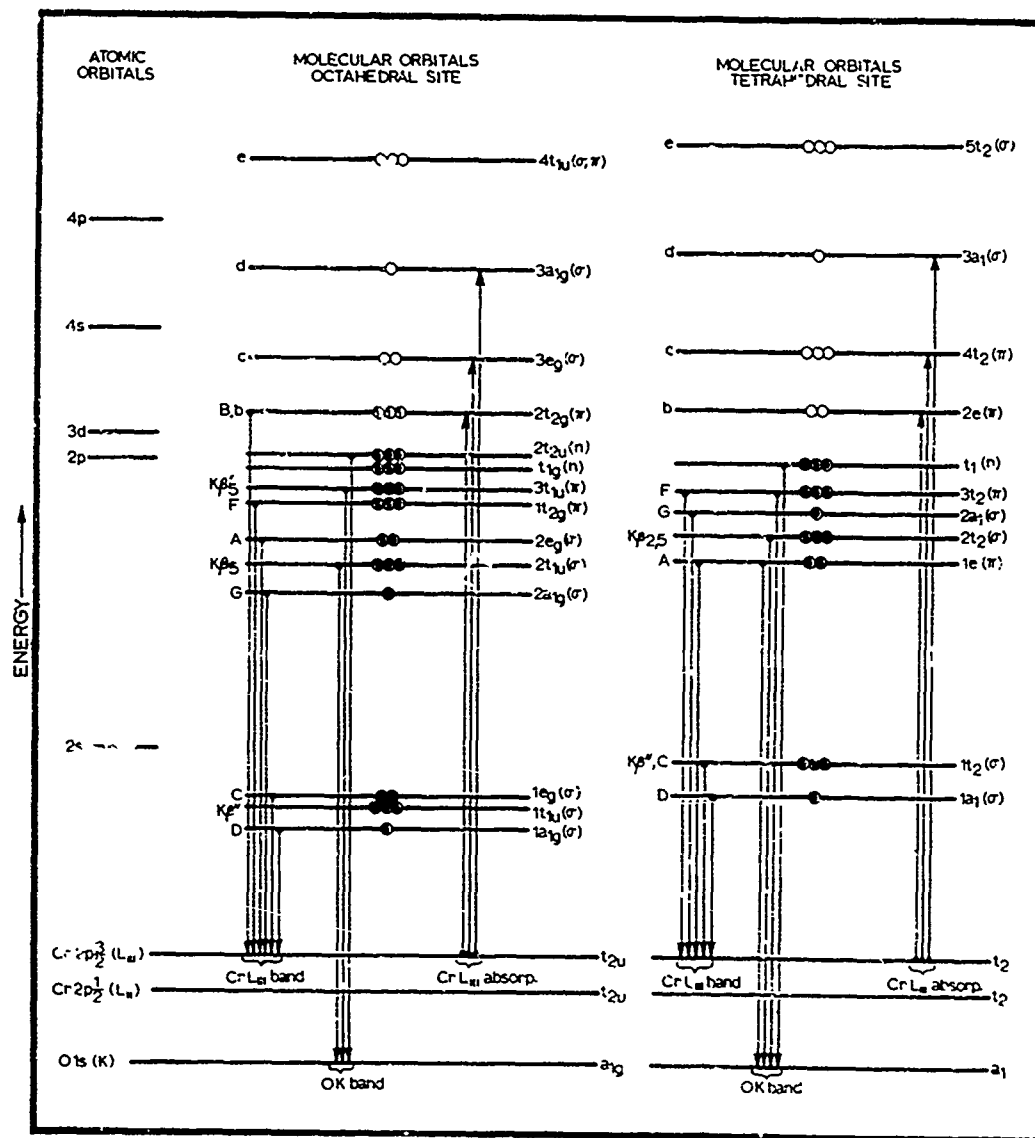
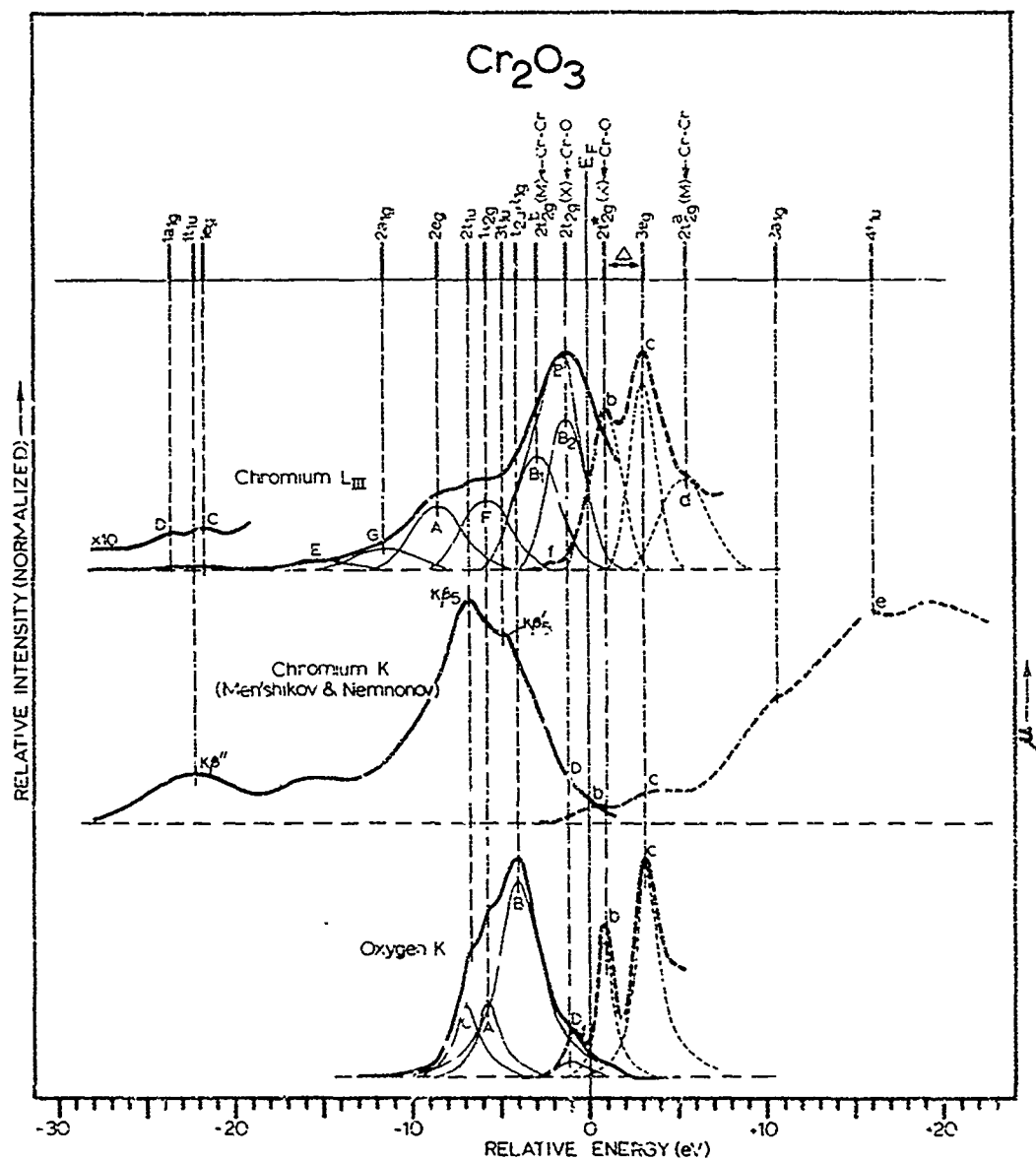


Figure 3. Schematic molecular-orbital energy-level diagrams for chromium in octahedral and tetrahedral symmetry sites with oxygen anion. Vertical lines indicate electron transitions most likely to contribute to specific spectra. Diagrams adapted from Ballhausen and Gray (Reference 17). Not drawn to scale.



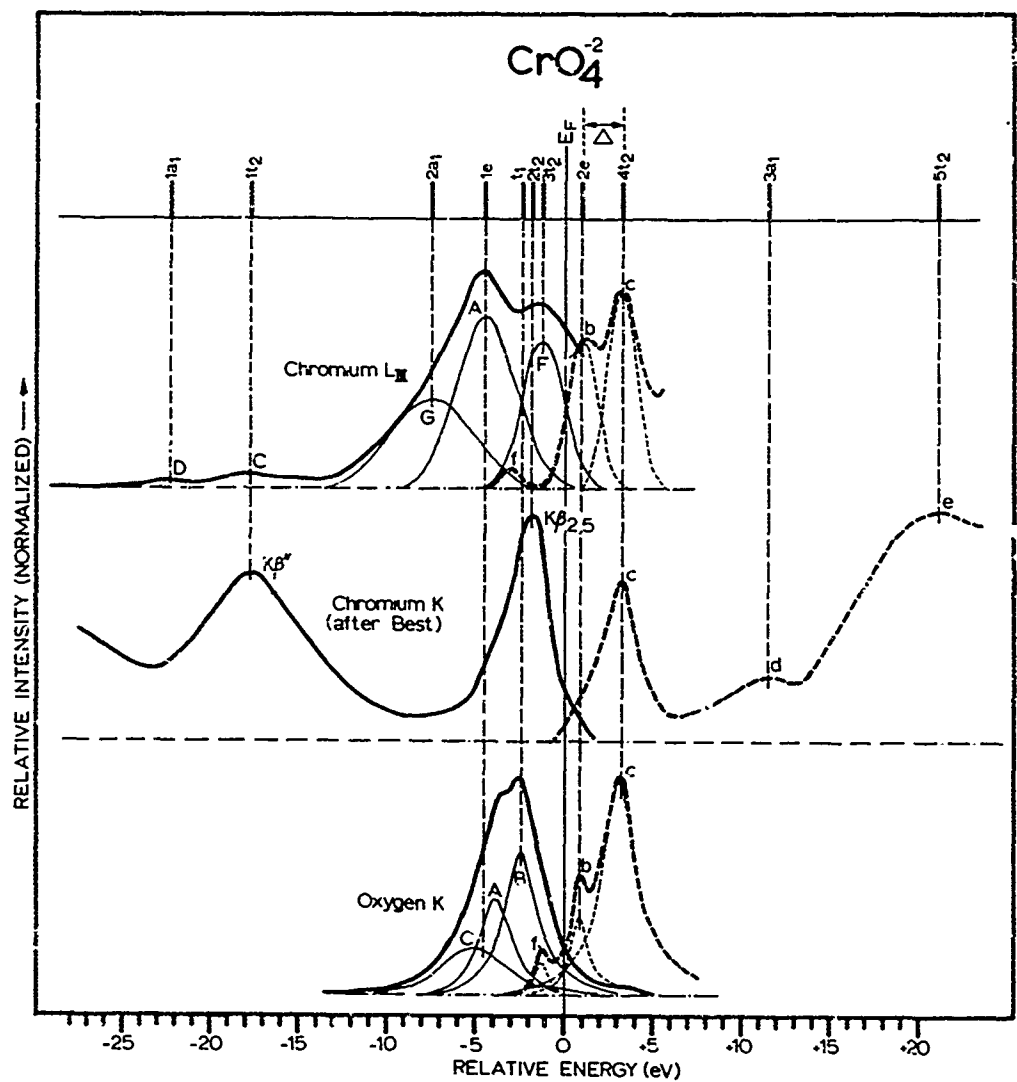


Figure 5. Empirical deduction of MO structure of CrO_4^{2-} by combining the chromium L, chromium K, and oxygen K x-ray band spectra from Na_2CrO_4 .

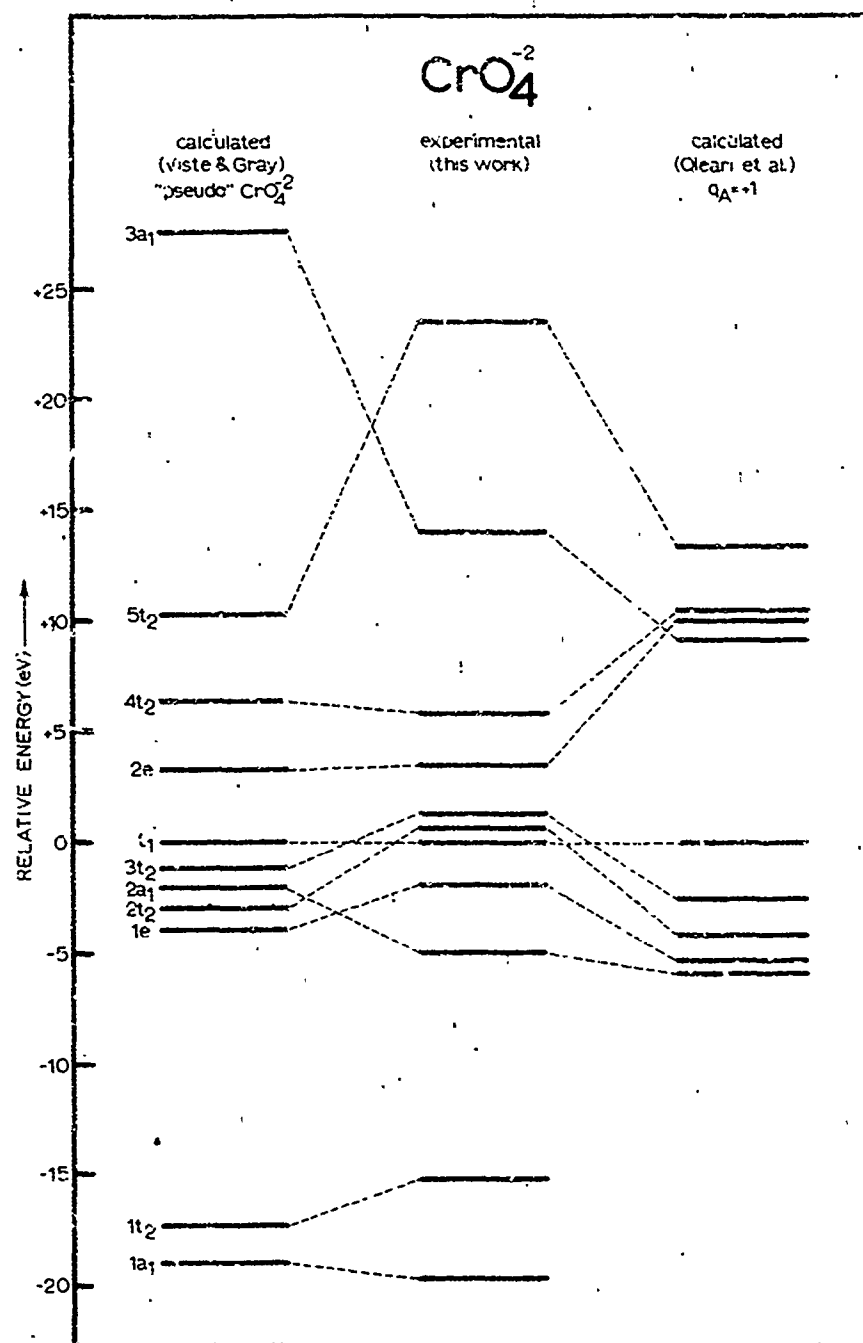


Figure 6. Comparison of relative MO energy positions of CrO_4^{-2} determined in this work and calculated by Viste and Gray (Reference 35) and Oleari et al. (Reference 36). Zero of energy arbitrarily placed at t_1 nonbonding level to facilitate comparison.

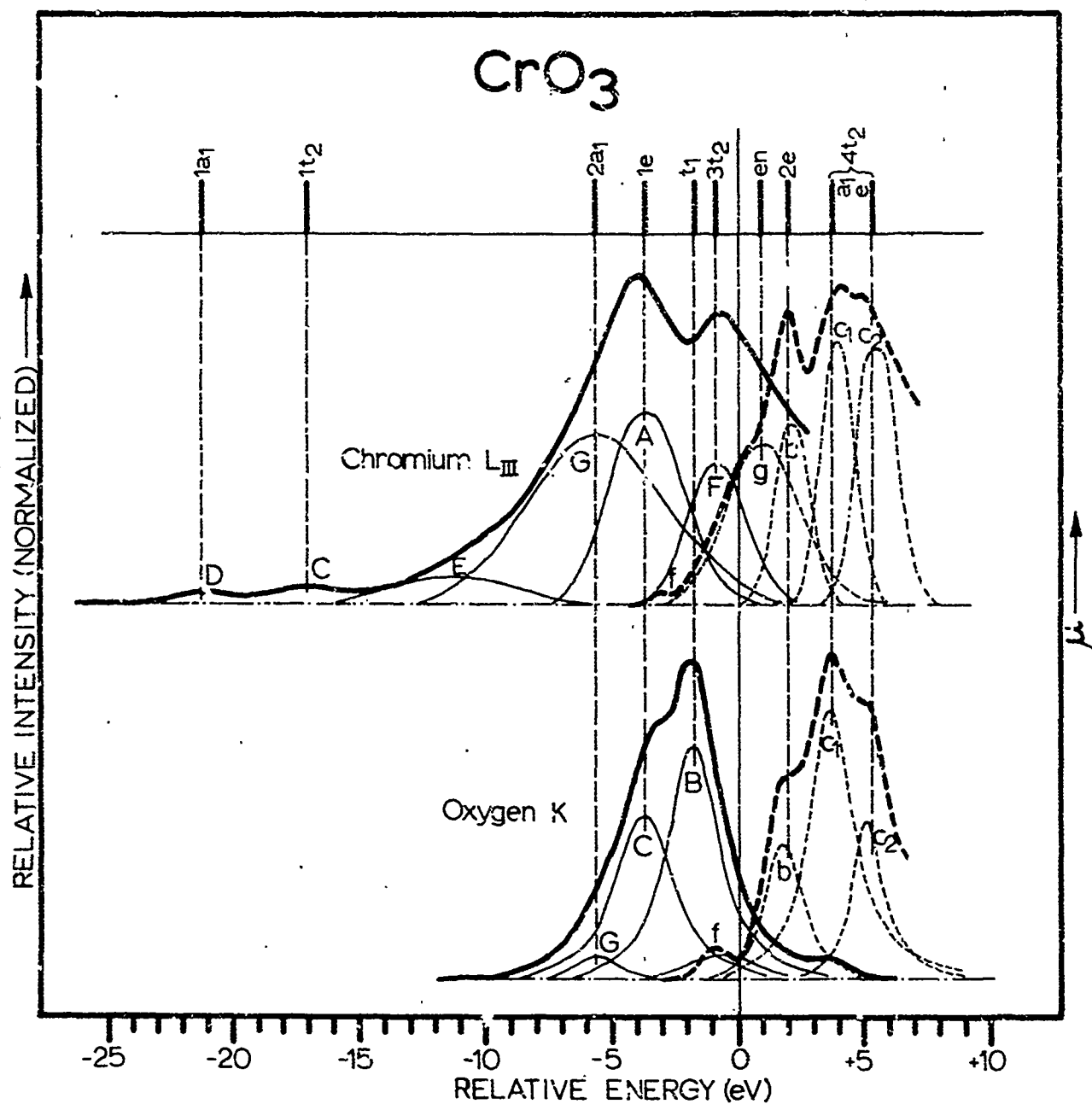


Figure 7. Empirical deduction of partial MO structure of CrO₃ by combining the chromium L and oxygen K x-ray band spectra.

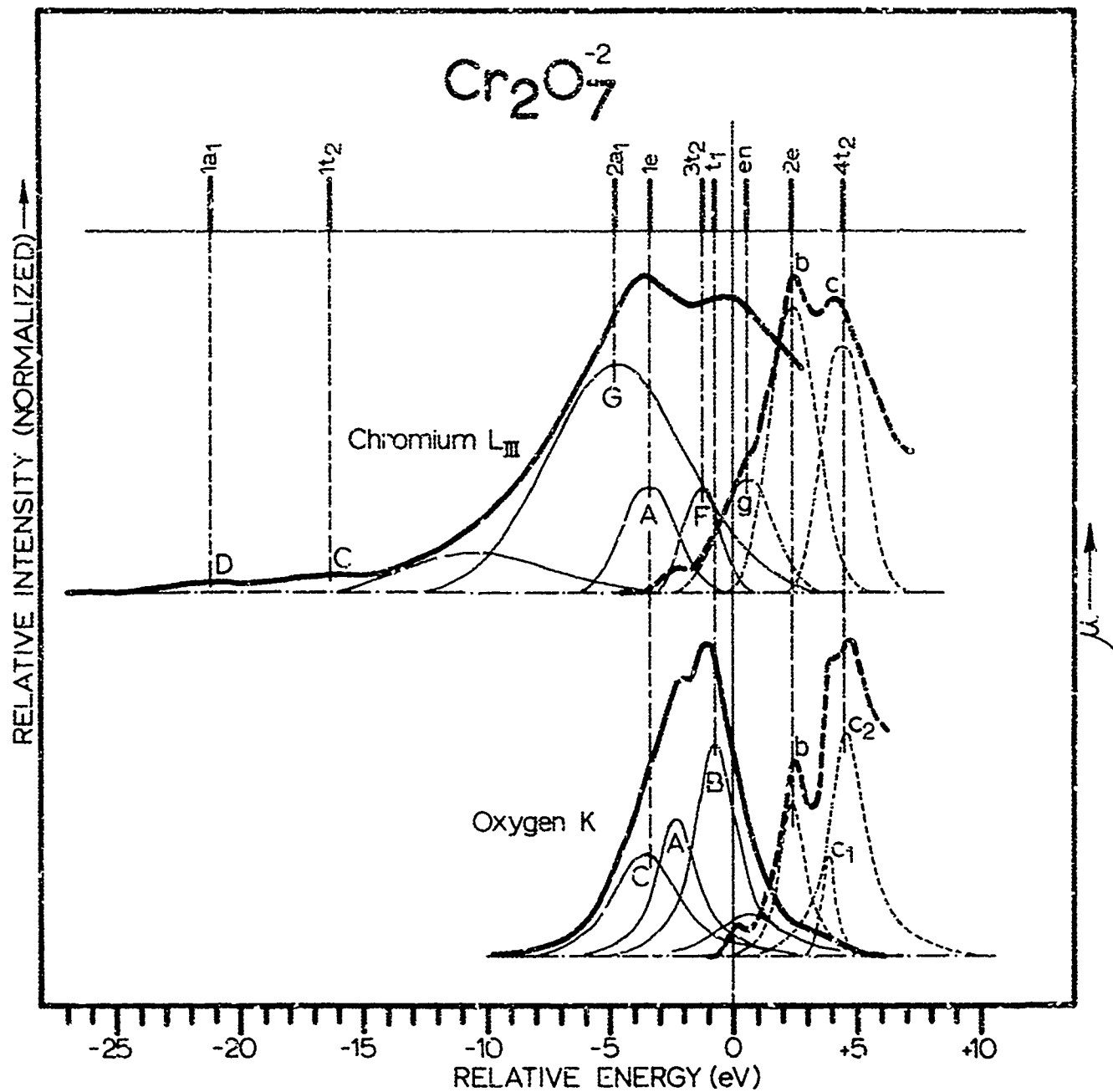


Figure 8. Empirical deduction of partial MO structure of $\text{Cr}_2\text{O}_7^{-2}$ by combining the chromium L and oxygen K x-ray band spectra from $\text{K}_2\text{Cr}_2\text{O}_7$.